

Xiaojing Sun · Xinyu Gong · Diangui Huang

## A review on studies of the aerodynamics of different types of maneuvers in dragonflies

Received: 16 September 2015 / Accepted: 8 November 2016 / Published online: 29 November 2016  
© Springer-Verlag Berlin Heidelberg 2016

**Abstract** In the recent decades, biomimetic robots have attracted scientific communities' attention increasingly, as people try to learn from nature in which exist astonishing and uniquely evolved mechanisms shown by very species. Dragonfly, as such one example, demonstrates unique and superior flight performance than most of the other insect species and birds. Researchers are obsessed with the aerodynamic characteristics of an in-flight dragonfly as two pairs of independently controlled wings provide them with an unmatchable flying performance and robustness. In this paper, an extensive review of recent studies related to the flight aerodynamics of dragonflies has been conducted. The main research findings about effect of the motion parameters and body attitude on the resulting aerodynamic forces and power requirements in different flight modes of a dragonfly are summarized. Particular attention is given to functional characteristics of dragonfly wings and the importance of mutual interaction between forewing and hindwing for its flyability. This article aims to bring together current understandings of dragonfly aerodynamics and thus has certain reference value to design and control of dragonfly-inspired biomimetic devices.

**Keywords** Dragonfly · Aerodynamic characteristics · Recent research progress · Biomimetic

### 1 Introduction

With the increasing advancement in the development of microelectromechanical devices, including microsensors, pumps, valves and micromotors, tiny robotic flyers, called micro-air vehicles (MAVs), they have drawn tremendous attention worldwide in recent years because of their popular applications ranging from civil search-and-rescue missions to military surveillance missions. Based on the mechanism of generating lift, MAVs can be generally classified into three kinds: fixed, rotary and flapping wing. For flapping wing MAVs, a great number of them have been designed and developed from inspiration from flapping flights of insects and birds [1]. Among those instinctive flyers, the flight capabilities of dragonflies are prodigious as they have two sets of wings, which allow them to perform unique juggling maneuvers including hovering, powerful ascending flight, making turns rapidly, flying sideways and even gliding. By mimicking their structures and sensory mechanisms, engineers have designed different types of dragonfly-inspired micro-aerial vehicle which continues to evolve with the continuous development of bionic technology [2–6]. It assumes that the superior flight performance of dragonflies benefits from the relative motion and mutual flow interactions between two sets of their wings. Driven by a desire for the small size and high agility of biomimetic MAVs, extensive studies

---

X. Sun · X. Gong · D. Huang  
University of Shanghai for Science and Technology, Shanghai 200093, People's Republic of China

X. Sun · X. Gong · D. Huang (✉)  
Shanghai Key Laboratory of power energy in multiphase flow and heat transfer, Shanghai 200093, People's Republic of China  
E-mail: dghuang@usst.edu.cn

have been conducted on actual dragonflies to understand how wings work and why they are so well suited to generate the diversity, the elegance and the power of biological movements.

In general, research on dragonflies has gone through two phases. In the first stage (the early 1990s and earlier), various works done by researchers including Azuma [7,8], May [9], Wakeling [10–12] and Alexander [13–15] laid the foundation for the study of aerodynamics of dragonfly flight. Those researchers captured images of dragonflies in flight from cameras and started to analyze the wing kinematic parameters including angle of attack and movements of two pairs of wings at different flight maneuvers. Experimental tools were used to measure aerodynamic forces generated by the moving wings, and various relationships between wings' movement patterns and force production were able to be analyzed [16]. References [17–20] are some other examples of much earlier work on dragonfly aerodynamics. The second phase started from the late 1990s until now. During this period, a large body of research exists and continues to explore all aspects of the biological significance of dragonfly behavior, focusing especially on lift- and thrust-generating mechanisms in dragonflies, such as Russell [21,22], Thomas [23], Wang [24–26] and Sun [27–31]. These studies indicate that two pairs of wings are not only responsible for producing the mechanical power required for sustained flapping flight in dragonflies, but can also be responsible for improving aerodynamic efficiency by the wing-wing interactions [31,32], which is historically defined as the ratio of the average power made good (the product of force produced by the wings in the direction of flight and airspeed) and the average power spend. Without a doubt, there has been rapid progress made in advancing researchers' understanding of dragonfly aerodynamics thanks to the recent developments in high-speed videography and tools for computational and mechanical modeling. A summary of some of the work the most highly cited researchers did is further detailed in subsequent sections of the paper.

Based on the extensive literature review, this paper aims to summarize the basic physical principles underlying flapping flight in dragonflies, results of recent experimental and computational results concerning the aerodynamics of dragonfly flight, as well as the approaches undertaken to study the phenomenon. The main purposes of this paper are to identify possible knowledge gaps, present proposals for further research and also provide valuable information for those interested in pursuing biomimetic technologies based on nature's designs.

## 2 Flight characteristics of a dragonfly

### 2.1 Schematic representations of flapping motion

Flapping flight is more complicated than flight with fixed wings because of structural movement and the resulting unsteady fluid dynamics. With two pairs of wings which can beat in phase or out of phase, dragonflies are high-performance fliers. A dragonfly in free flight is capable of gliding, hovering in midair, rapid acceleration and sustained forward flight [33]. Therefore, dragonflies can easily avoid hidden predators thanks to these many different flight modes.

In order to learn about the fluid dynamics associated with different flight modes of a dragonfly, the periodic cycle of their wing motion is widely studied using simplified model as shown in Fig. 1. The black dot represents the leading edge of the wing, the thick black line denotes the instantaneous position of wing section, the dash line shows the wing path, and a filled arrow head indicates wing motion [34–36]. However, some researchers suggest that dragonfly actually flaps its wings along an inclined stroke plane with respect to the longitudinal body axis [33,37,38], as shown in Fig. 2. Therefore, the simplified 2D models of dragonfly wings, which perform their flapping in a stroke plane inclined with respect to the horizontal level, become more widely accepted and used as represented in Fig. 3.

### 2.2 Motion parameters of the wing flip

Figure 4a gives the definition of the stroke plane of the wing used often in dragonfly research. In Figure 4a, point  $B_1$  indicates the wingbase of the left forewing of a dragonfly. Through  $B_1$ , a horizontal plane is drawn and acts as a reference. Another point  $T_1$  at the wingtip is also defined, and many researchers normally use pterostigma on the wing of a dragonfly as point  $T_1$  in order to facilitate the analysis. The leading edge of the wing is thus determined by the line  $B_1 - T_1$ . In addition, there exist upstroke limit and downstroke limit of the motion of the wings during the flapping cycle which are, respectively, denoted by  $T_{1H}$  and  $T_{2L}$ . As a result, a plane determined by the three points  $B_1$ ,  $T_{1H}$ , and  $T_{1L}$  is defined as the wing-stroke plane. As the wing moves,

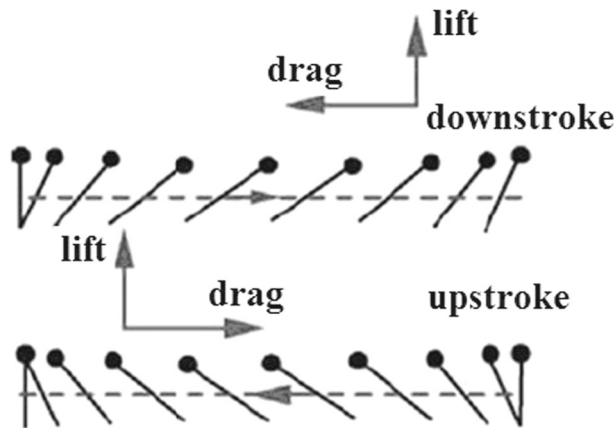


**Fig. 1** Schematic diagram of flapping motion of the 2D dragonfly's wing section along a horizontal stroke plane [39]

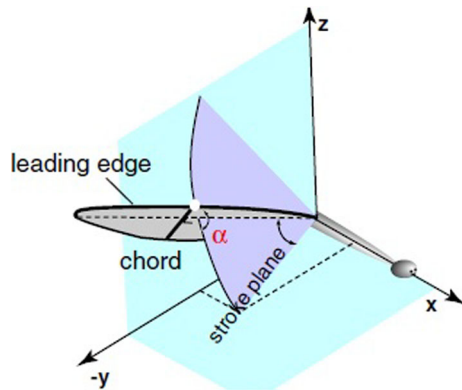


**Fig. 2** Diagram of dragonfly's wing coordinate system [22]

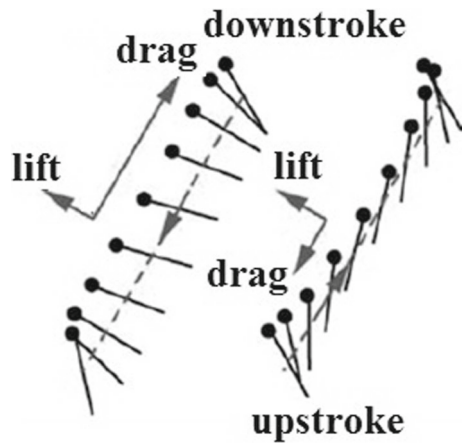


**Fig. 3** 2D projection of wing flapping motion along an inclined stroke plane in one cycle [39]

time-varying instantaneous angle  $\varphi$  between line  $B1 - T1$  and reference plane is called flapping angle and its maximum amplitude is represented by  $\phi$ . In addition, the stroke plane angle  $\theta$  measures the inclination of the stroke plane, relative to the reference plane.  $\beta$  is the angle between the wing chord line (line between the leading edge and the trailing edge) and the stroke plane.  $\gamma$  is the angle between the longitudinal axis of the dragonfly's body (a straight line extending from the tip of the head to the tip of the tail [7]) and the horizontal.  $\alpha$  is the angle of the orientation of the stroke plane with respect to the direction the dragonfly is facing. These parameters are clearly demonstrated in Fig. 4b.

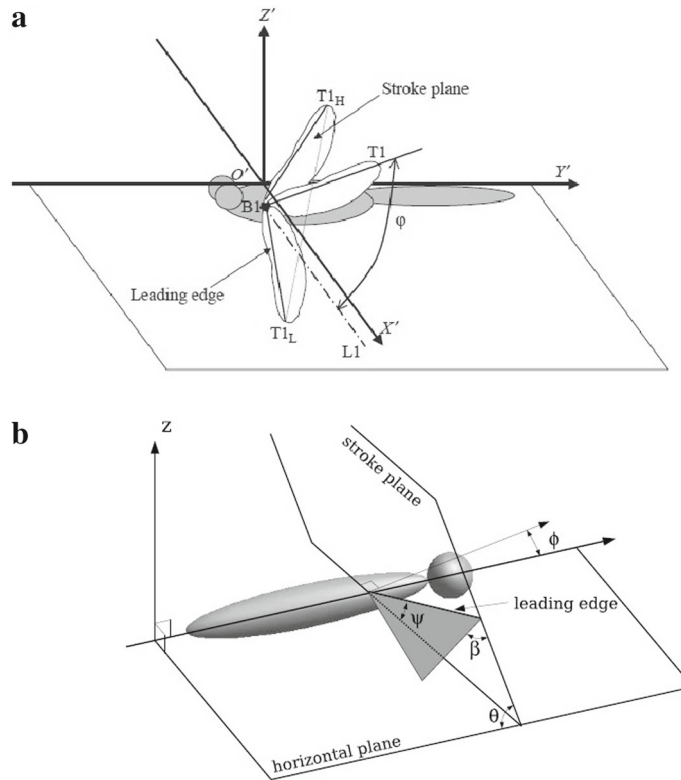


**Fig. 4** Definition of stroke plane and parameters used to describe the three-dimensional (3D) wing motion **a** [40], **b** [21]

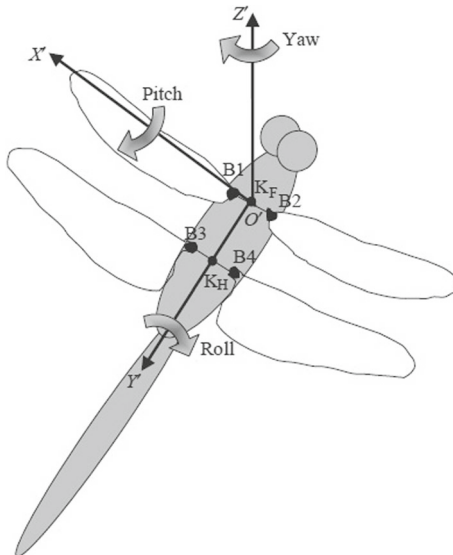


**Fig. 5** Illustration of the local body-fixed coordinate system and three-dimensional rotational movement of a dragonfly in flight [40]

Except spatial coordinate system, a local body-fixed coordinate system illustrated in Fig. 5 is also used to describe rotation of dragonfly wings. According to Fig. 5, a dragonfly in flight can be free to rotate in three dimensions: pitch, head up or down about an axis running from wing to wing; yaw, head left or right about an axis running up and down; and roll, rotation about an axis running from head to tail.

For dragonfly studies, two-dimensional (2D) kinematic analysis has been widely adopted as a 2D dragonfly model is believed to be able to represent the same phenomenon as the 3D model and capture the essential

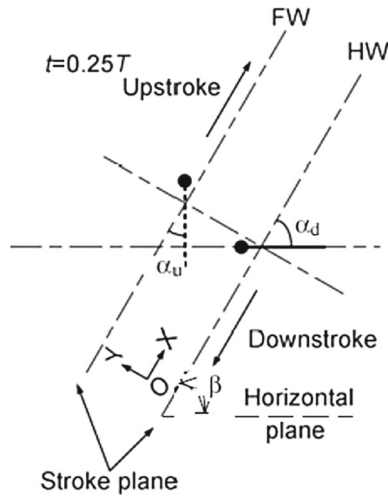


**Fig. 6** The position relationship between the 2D wing section of the fore (FW, the dash line with a black dot) and hind (HW, the solid line with a black dot) wings at  $t/T = 0.25$  [41]

physics [38]. Therefore, understanding of the parameters utilized to assess 2D flapping wing fluid physics is equally important. Figure 6 demonstrates an example of the 2D flapping wing model used in Ref. [16]. In Fig. 6, two thick straight lines with black dot represent the forewings on upstroke and hindwings on downstroke, respectively. It is accepted that no matter fore or hindwings,  $\alpha_u$  is the upstroke angle of attack of the wing and  $\alpha_d$  is the downstroke angle of attack of the wing.

### 2.3 Aerodynamic forces generated by the flapping wing

Flapping wings enable flying dragonflies to generate elevated aerodynamic forces. For instance, in the case of forewings, lift and drag are the forces perpendicular and parallel to the stroke plane, denoted by  $l_f$  and  $d_f$ . However, the two most important forces acting on the dragonfly are the vertical component ( $V_f$ ) that balances its body weight and the horizontal component ( $T_f$ ) that moves it forward.  $V_f$  and  $T_f$  are expressed using the lift and drag components [42]:

$$V_f = l_f \cos \theta + d_f \sin \varphi \sin \theta \quad (1)$$

$$T_f = l_f \sin \theta - d_f \sin \varphi \cos \theta \quad (2)$$

In most cases, the normalized coefficients  $C_{V,f}$  and  $C_{T,f}$  are used more often if the areas of both the forewing ( $S_f$ ) and hindwing ( $S_h$ ) are determined.

$$C_{V,f} = V_f / [0.5\rho V_\infty^2 (S_f + S_h)] \quad (3)$$

$$C_{T,f} = T_f / [0.5\rho V_\infty^2 (S_f + S_h)] \quad (4)$$

Accordingly, the total vertical force  $V$ , total vertical force coefficient  $C_V$ , total thrust force  $T$  and total thrust force coefficient  $C_T$  are the sum of the contributions from the fore- and hindwings.

$$V = V_f + V_h \quad (5)$$

$$T = T_f + T_h \quad (6)$$

$$C_V = C_{V,f} + C_{V,h} \quad (7)$$

$$C_T = C_{T,f} + C_{T,h} \quad (8)$$

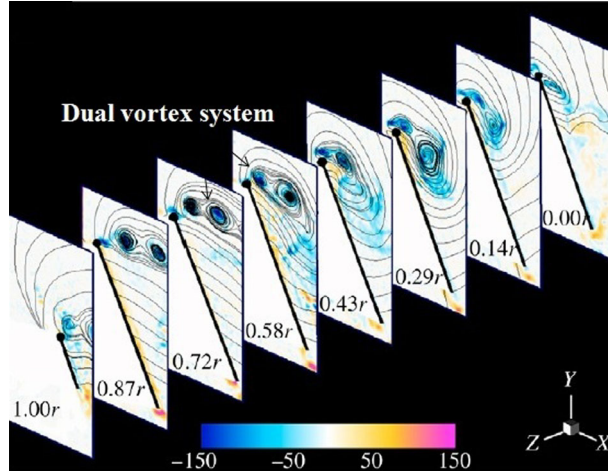


**Fig. 7** Dual vortex system captured by DPIV at mid-downstroke ( $0.25T$ ). The black thick line denotes wing section, and the solid-dot represents the leading edge. The slices are placed by 15 mm and are all perpendicular to the spanwise direction [36]

## 2.4 Formation of the leading-edge vortex on dragonfly wings

Entomologists generally recognized that the elevated aerodynamic performance of the flapping flight of insects has been attributed in part to the generation and maintenance of a stable region of vorticity known as the leading-edge vortex (LEV). Aerodynamically, it is well known that leading-edge vortices create a lower-pressure region on suction surface of wing, which greatly increases the force production [43,44]. In order to identify the role of LEVs in lift generation in different flight modes of a dragonfly, some researchers tried to study the flow structure of LEV on its flapping wings by using various visualization techniques. Using digital particle image velocimetry (DPIV) optical technique and a model dragonfly wing, Lu and coworkers [36] captured continuous images of vortex evolution along the spanwise direction from the wing base to the tip. As can be seen in Fig. 7, their images demonstrate the existence of a dual LEV system on flapping wings when the tested angle of attack and  $R_e$  reached certain high levels.

Thomas et al. [23] used smoke visualizations to observe the formation and structure of the leading-edge vortex in the free flapping flight of a dragonfly. Through their photographs, one of which is displayed in Fig. 8, the development of LEV during both the downstroke and the upstroke can be better understood. Fig. 8a shows the end of the upstroke, while the tested dragonfly did not experience roll and yaw. Figure 8b shows the beginning of the downstroke of the flapping cycle, and the yellow arrow shows the approximate location of a LEV that occurs on the forewing. In the meantime, the dragonfly rolls and yaws to the left. In (c), the LEV grows and its center bulges toward the midline at the yellow arrow, indicating the occurrence of a spanwise flow. From the following images (d)–(h), both LEV and spanwise flow increase during downstroke of the wings. The LEV persists on the surface of the wing even during the bottom of downstroke (i) and early upstroke (j). Thomas et al. also conducted flow visualizations around a tethered dragonfly. According to their pictures presented in Fig. 9a, b, a vortex formed near the leading edge of forewing grows in strength and, to some extent, is transferred from forewing to hindwing at the end of downstroke. Based on observations from these photograph frames, Thomas et al. identified that the dynamic behavior of leading-edge vortices is closely related to the wing angle of attack and the dragonfly can take advantages of LEVs by adjusting the wing angle of attack over a wide range. In addition, they also confirmed that to what extent the main flow characteristics of interactions between flapping wings are able to be captured by 2D simulation.

Similarly, Hefler et al. [45] conducted particle image velocimetry (PIV) measurement of the air flow around a live dragonfly, while tethered and particular attention was paid on the effect of wing phasing. Their smoke visualization in Fig. 10 shows when dragonfly flaps its wings in phase, there exist a forewing leading-edge vortex and also a hindwing trailing-edge starting vortex on the first downstroke. They suggested that dragonfly uses in-phase flapping upon takeoff to generate downward momentum, a finding also reported by Alexander [46]. Tandem wings flapping in-phase work like one large wing, which creates both one LEV and one trailing-edge starting vortex on the forewing.

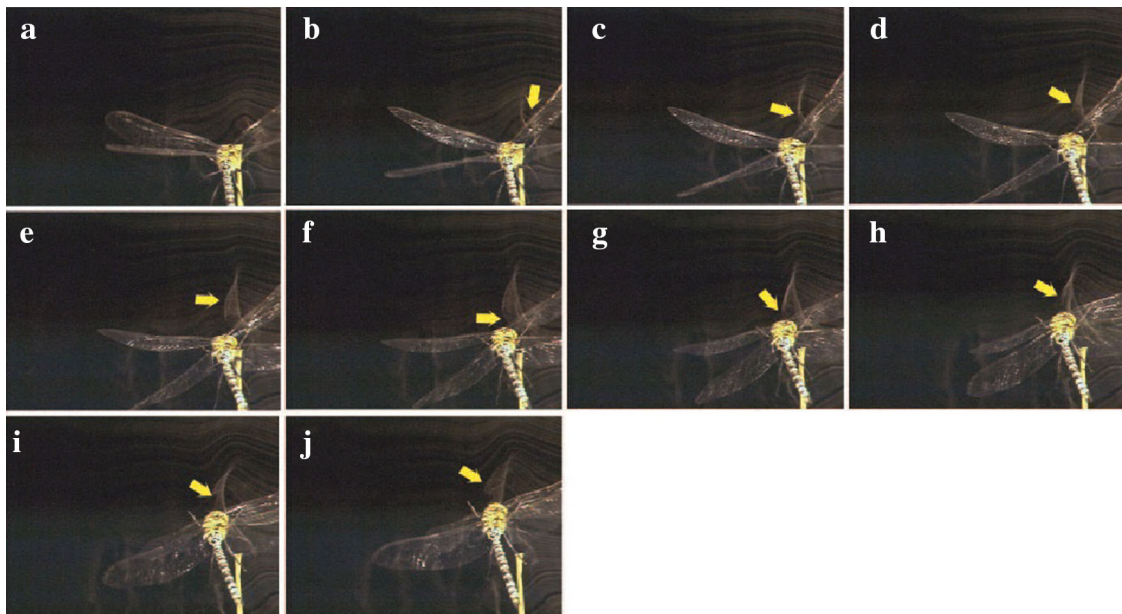


**Fig. 8** Free-flight smoke visualization showing the development of LEV on the wings of *Aeshna mixta* in counterstroking flight with increasing left roll and yaw and consequent side slip [23]

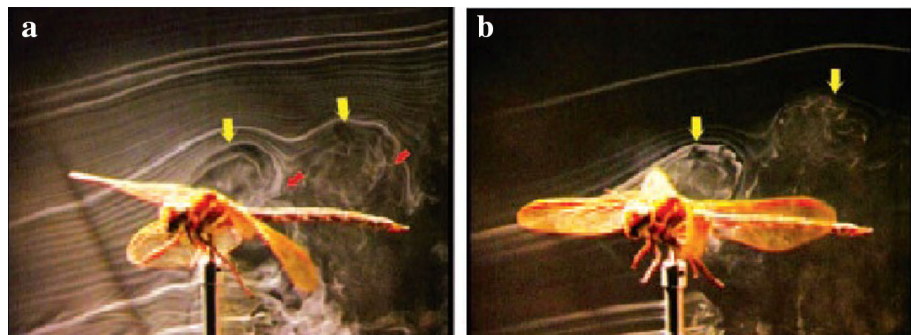


**Fig. 9** Two images showing convection of a fully developed leading-edge vortex [23]

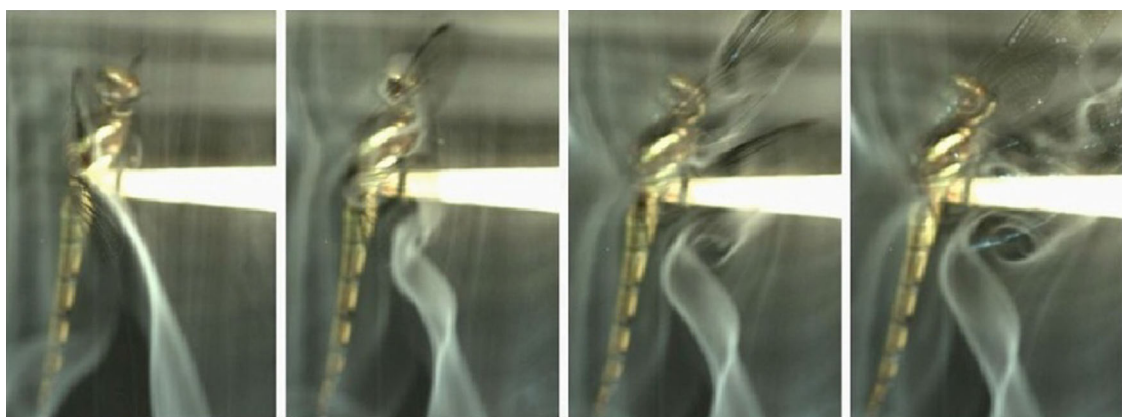


**Fig. 10** Vortex growth and shedding at the first downstroke of an in-phase flapping dragonfly [45]

**Table 1** Aerodynamic parameters of *Sympetrum sanguineum* measured during gliding flight [10]

Identity, air temperature (°C)	Glide angle (°)	Glide speed (m/s)	Backwards acceleration (m/s <sup>2</sup> )	Vertical acceleration (m/s <sup>2</sup> )	Lift:drag ratio <i>L/D</i>	Lift coefficient
SSan21, 37.2	-7.4 6.2	2.6 2.1	3.5 1.0	2.2 -6.7	6.3 2.2	0.56 0.20
SSan22, 39.4	15.4 26.9	1.6 2.0	4.4 3.2	-4.5 2.1	0.7 1.1	0.50 0.70
SSan24, 40.1	34.2 36.2 33.4	2.0 2.2 2.1	-1.1 -1.9 -1.0	-1.4 -1.8 7.8	2.0 2.4 1.7	0.53 0.43 0.93
SSan26, 33.8	10.6 3.5 0.9 26.4	2.4 2.1 1.3 1.9	3.2 3.3 1.5 1.8	-7.9 -5.8 -8.4 -7.4	0.4 1.1 0.9 0.5	0.06 0.20 0.20 0.09
SSan27, 32.6	13.5 8.4	0.8 1.9	3.6 3.1	-7.4 -5.3	0.4 1.1	0.61 0.33

With the rapid progress of CFD capability and computer power, a better understanding of force production and flow structure of the leading-edge vortex on flapping wings of a dragonfly can be gained with the aid of numerical analysis. Results from those studies are discussed in the following section.

### 3 The aerodynamics of different types of flight modes in dragonflies

In this section, recent studies on the aerodynamics of different types of maneuvers in dragonflies are reviewed. The main research findings on the mechanisms of high aerodynamic forces generation and power requirements of dragonfly flying in different flight modes are thus assessed.

#### 3.1 Gliding flight

Gliding is part of dragonflies' natural flight repertoire, and it is reported that the dragonfly can glide 40 chord lengths over one complete wing beat [47]. In dragonfly's gliding flight, there is no relative motion of its forewings and hindwings and little effort is required for the dragonfly to stay in the air for long periods. Gliding flight is the simplest form of flight [48], and thus under such steady condition, gliding performance like the resultant forces acting on the wings of a dragonfly can be easily measured and analyzed [10]. In addition, according to some researchers [49–51], the frequency of the gliding flight of dragonflies tends to increase during hot weather as dragonflies can take advantage of convective cooling by gliding quickly through the air without additional heat production by their flight muscles. May [52] further reported that the wingbeat frequency and flight speed may decline, while the proportion of time spent on gliding increases with increasing the ambient temperature.

Wakeling and Ellington [10] filmed the free gliding flight of the dragonfly and provided a set of aerodynamic parameters which are given in Table 1 and estimated from the performance of *Sympetrum sanguineum*, a European species of dragonfly. Based on these observations and data samples, they found that dragonflies glide within a vertical plane and do not turn while gliding. During glide periods, there exist the acceleration component along the dragonfly flight path and the vertical component of acceleration, i.e., the two forces act in the direction of the accelerations. Thirteen of gliding flight sequences were caught on camera and analyzed by Wakeling and Ellington [9]. The aerodynamic characteristics of these glide sequences recorded for *Sympetrum sanguineum* are summarized in Table 1. As they assumed that all the lift was produced by the wings and not the body, the lift coefficient given in Table 1 thus represents a mean value for both the forewings and the hindwings. According to Table 1, there existed backward acceleration and vertical acceleration during gliding flight. Higher lift coefficients produced by the wings were occurred when the dragonfly accelerated upward (positive values in Table 1) during gliding flight. In addition, these dragonflies seemed to be more likely to glide at a large angle from the horizontal at high temperature. These measured aerodynamic characteristic values will provide good features for comparison with numerical simulations.

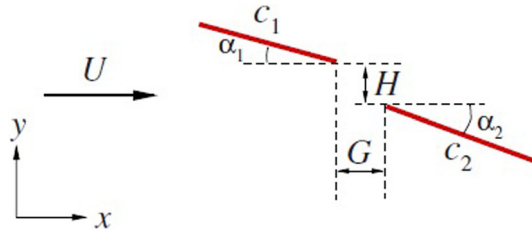


**Fig. 11** 2D dragonfly wing model in gliding flight used by Zhang and Lu [53], in which the red left line indicates forewing and the red right line represents hindwing. (Color figure online)

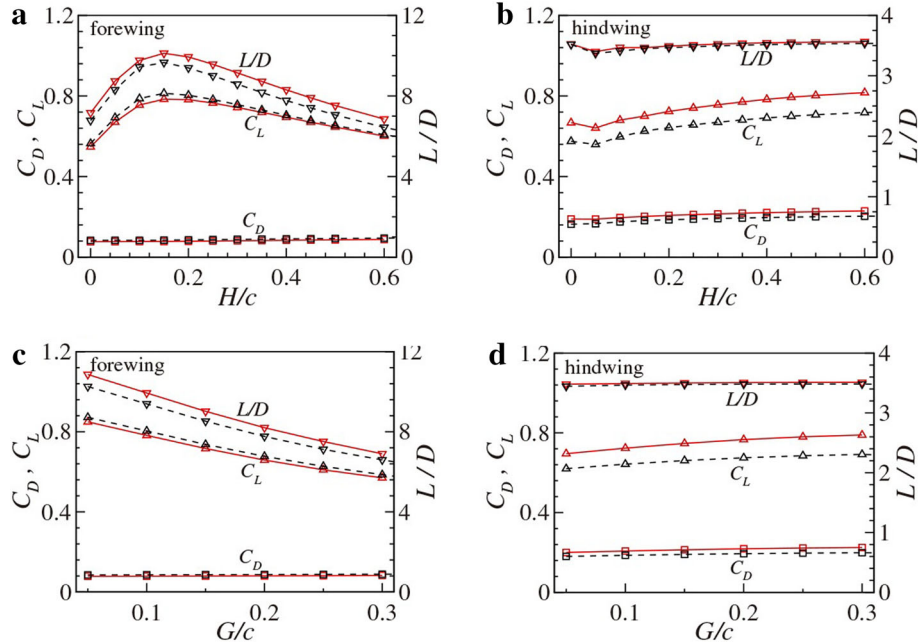


**Fig. 12** Time-averaged lift ( $C_L$ ) and drag ( $C_D$ ) coefficient and their ratio for  $\alpha_1 = 2^\circ$ ,  $\alpha_2 = 12^\circ$ , and  $R_e = 1000$ . **a** Forewing at  $G/c = 0.1$ . **b** Hindwing at  $G/c = 0.1$ . **c** Forewing at  $H/c = 0.2$ . **d** Hindwing at  $H/c = 0.2$ . The red and black symbols represent  $C_L(\Delta)$ ,  $C_D(\square)$  and  $L/D$ (inverter triangle). The solid red and dashed black lines denote  $c_1/c_2 = 0.9/1.1$  and  $1/1$  [53]. (Color figure online)

2D numerical analysis of gliding flight of a dragonfly wing was conducted by Zhang and Lu [53], and their numerical model is shown in Fig. 11, in which two thick red lines represent the fore- (left) and hindwing (right) of a dragonfly during gliding, the angle of attack  $\alpha_1$  and  $\alpha_2$ ;  $H$  and  $G$  are the vertical and horizontal distances of the forewing trailing edge and hindwing leading edge.

Figure 12 illustrates the variations of time-averaged lift ( $C_L$ ) and drag coefficient ( $C_D$ ) and their ratios with  $H$  and  $G$ . According to this result, it can be seen that  $C_D$  of the gliding dragonfly wing basically does not vary in relation to the changes in  $H$  or  $G$ , especially for the forewing whose values of  $C_D$  appear to remain constant. This finding is consistent with Xiao [54, 55] who studied the dragonflies in hovering and acceleration mode and found that flow field around the forewing is hardly affected by condition changes behind it. However, the  $C_D$  of hindwing of dragonfly shown in Fig. 12b, d slightly increases with increasing  $H$  or  $G$ . The influence of forewing on the hindwing should be weakened as  $H$  or  $G$  increases, indicating a larger distance between the forewing and hindwing pairs. The increase in the hindwing drag coefficient at higher  $H$  or  $G$  suggests that the interactions between forewing and hindwing have no beneficial effects in improving thrust production. From the lift coefficient graph shown in Fig. 8, it can be seen that with increasing  $H$ , there exists a maximum lift coefficient ( $C_{L(\max)}$ ) for the forewing, while the lift coefficient on hindwing shows a gradual increasing tendency. If  $G$  increases, but  $H$  is fixed, the values of the lift coefficient of forewing show a gradual decrease, and conversely, the lift coefficient of hindwing increases slightly.

According to Zhang and Lu, not only the distance but also the wing posture affects the aerodynamic forces generated by the dragonfly while gliding. Therefore, they also studied the influence of the angle of attack  $\alpha$

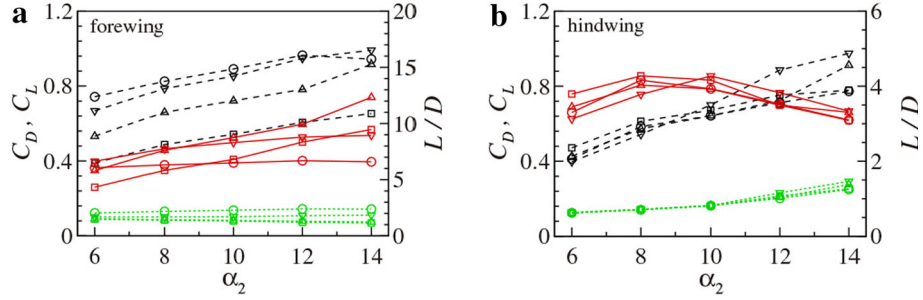


**Fig. 13** Time-averaged lift ( $C_L$ ) and drag ( $C_D$ ) coefficient and their ratio ( $L/D$ ) for  $H/c = 0.2$ ,  $G/c = 0.1$ ,  $c_1/c_2 = 0.9/1.1$ , and  $R_e = 1000$ : **a** forewing; **b** hindwing. The lines represent  $C_L$  (dashed black lines),  $C_D$  (dotted green lines), and  $L/D$  (red solid lines) and the color symbols  $\alpha_1 = 0^\circ$ (square),  $2^\circ$ (triangle),  $4^\circ$ (inverter triangle), and  $6^\circ$ (circle) [53]. (Color figure online)

**Table 2** Zhang and Lu's comparison results of the forces for the forewing/hindwing interaction and the corresponding isolated wing case at  $\alpha_1 = 2^\circ$ ,  $\alpha_2 = 12^\circ$ ,  $c_1/c_2 = 0.9/1.1$ ,  $H/c = 0.2$ , and  $G/c = 0.1$ . The superscript  $i$  denotes the isolated wing [53]

	$C_D$	$C_L$	$L/D$	$C_D^i$	$C_L^i$	$L^i/D^i$
Forewing	0.079	0.782	9.899	0.097	0.168	1.732
Hindwing	0.207	0.723	3.493	0.264	0.958	3.629
Total	0.286	1.505	5.262	0.361	1.126	3.119

of the wing as changes in  $\alpha$  cause greater change in the effective wing area used for generating lift. Based on their results given in Fig. 13, it is found that the  $\alpha_1$  variation has only a major effect on the lift coefficient of forewing. But the lift coefficients of both fore- and hindwing increase with the increase of  $\alpha_2$ . In addition, the changes in  $\alpha_2$  have no effect on the thrust of forewing, whereas the thrust of hindwing has an obvious increase when it is greater than  $10^\circ$ . Zhang and Lu also calculated the drag and lift coefficients of fore- and hindwings which are coupled together and compared the results with those on an isolated wing. They summarized their comparison results in Table 2. It can be seen that compared to an isolated wing, the interaction between fore- and hindwings considerably increases the total lift of both wings and thus is of crucial significance in dragonfly gliding flight. In addition, based on their results, the interactions between the two wings seem to have profound effects on the aerodynamic forces acting on the forewing, resulting in a relatively large lift-to-drag ratio.

### 3.2 Hovering flight

Hovering is a flight mode usually applied by dragonflies when they spot prey. In hovering flight, the dragonfly can maintain stationary position over a reference point on the surface and only make slight adjustments to body posture for prey capture [56]. While hovering, the motion of a dragonfly's wings is mainly confined to an inclined stroke plane [57, 58] and forewings beat  $180^\circ$  out of phase with the hindwings [59, 60] although both sets of wings flap at the same rate. In this way, only lift force sufficient to balance the weight of the dragonfly is produced and minimum amount of power is expended to stay airborne, allowing the dragonfly to conserve energy while hovering in place [22, 61].

Xiao [54] studied hovering flight conditions of a dragonfly by numerically analyzing two pitching and plunging NACA 0012 airfoils in tandem formation which is shown in Fig. 14.  $H_0$  is heave amplitude,  $\alpha_0$  is pitch amplitude, and  $\Delta L$  is the longitudinal spacing between fore- and hindwings.

The equations of motion of 2D airfoils oscillating in pitch and plunge are given as below, where the subscript  $f$  refers to the forewing and the subscript  $h$  means the hindwing.

$$H_f(t) = H_0 \cos(\omega t) \quad \alpha_f(t) = \alpha_0 \cos(\omega t + \varepsilon) \quad (9)$$

$$H_h(t) = H_0 \cos(\omega t - \gamma_d) \quad \alpha_h(t) = \alpha_0 \cos(\omega t + \varepsilon - \gamma_d) \quad (10)$$

In the above equations,  $\omega$  is angular velocity of oscillating airfoil,  $\varepsilon$  is the phase difference between the pitch and plunge motions, and  $\gamma_d$  is the phase difference between forewing and hindwing. In hovering flight,  $\gamma_d$  is  $180^\circ$ . Evolution of the unsteady vortex structures around two tandem airfoils is displayed in Fig. 15. According to Xiao's results, a vortex is formed on the lower surface of the forewing at the top of upstroke. During downstroke

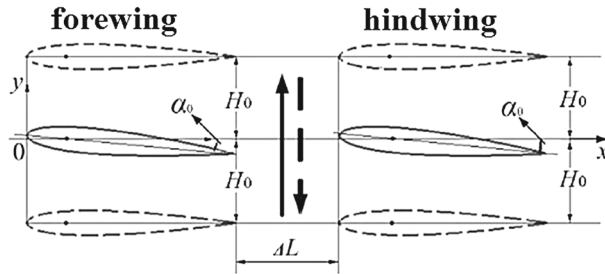


**Fig. 14** The arrangement of two airfoils in tandem [54]

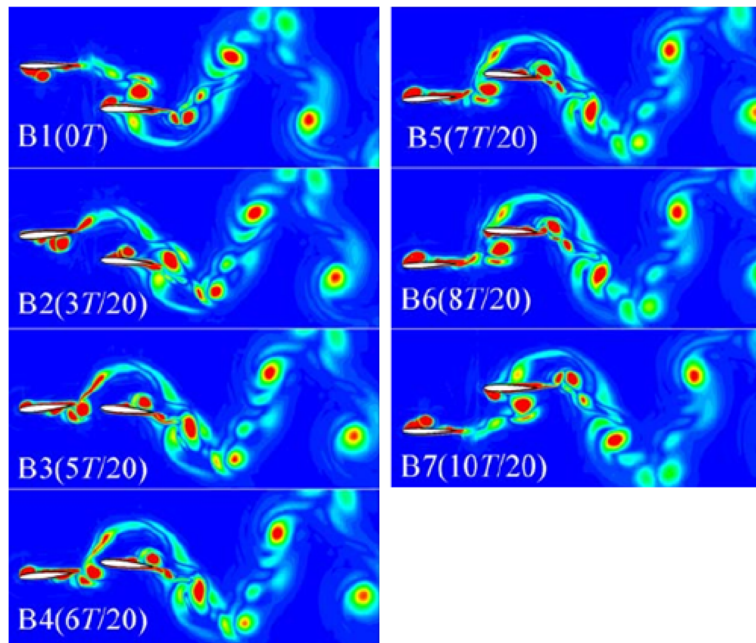


**Fig. 15** 2D vorticity contours around the flapping wings of a dragonfly in hovering flight [54]

of the forewing, the vortex continues to move toward the trailing edge of the wing flap and finally shed into the wake. Meanwhile, a leading-edge vortex is formed on the upper surface of the forewing at time  $t = 5T/20$  and grows in size but remains attached to the surface of the wing throughout the downstroke. The presence of the attached, leading-edge vortex contributes an additional region of low pressure on the upper surface, resulting in the high lift force found in insects and hummingbirds [62]. Xiao's results proved that to achieve hovering, LEV plays a vital role in terms of aerodynamic performances of the dragonfly's wings. In addition, it can be seen from Fig. 15 that flow field around the forewing is hardly affected by the flapping motions of the hindwings. On the other hand, a leading-edge vortex first starts to form on the upper surface of hindwing at the beginning of its upstroke. As the upstroke progresses, the vortex moves along the surface and is eventually shed into the wake under the influence of the time-varying wake of flapping forewings. Until almost the end of the upstroke, a new leading-edge vortex is then produced on the lower surface of hindwing. Data presented in Fig. 15 are shown that the forewing–hindwing interaction is not very strong in dragonfly hovering mode.

Xie and Huang [63] conducted a more comprehensive study of the aerodynamics of dragonfly in hovering flight by simulation of two-dimensional (2D) tandem flapping wings in viscous flow. They used immersed boundary method and studied the influence of the phase difference of the wing motions and the inter-distance of the two wings on the generated lift. They found that as the spatial distance between the two wings increases, the interaction between two wings becomes less pronounced and the total lift generated by the wings is less varied with the phase difference. The same finding was also reported by Hu and Deng [64] who experimentally studied the wing–wing interaction mechanism using the PIV technique. By examining the vorticity fields around the flapping wings, Xie and Huang claimed that the interaction of two wings of a hovering dragonfly

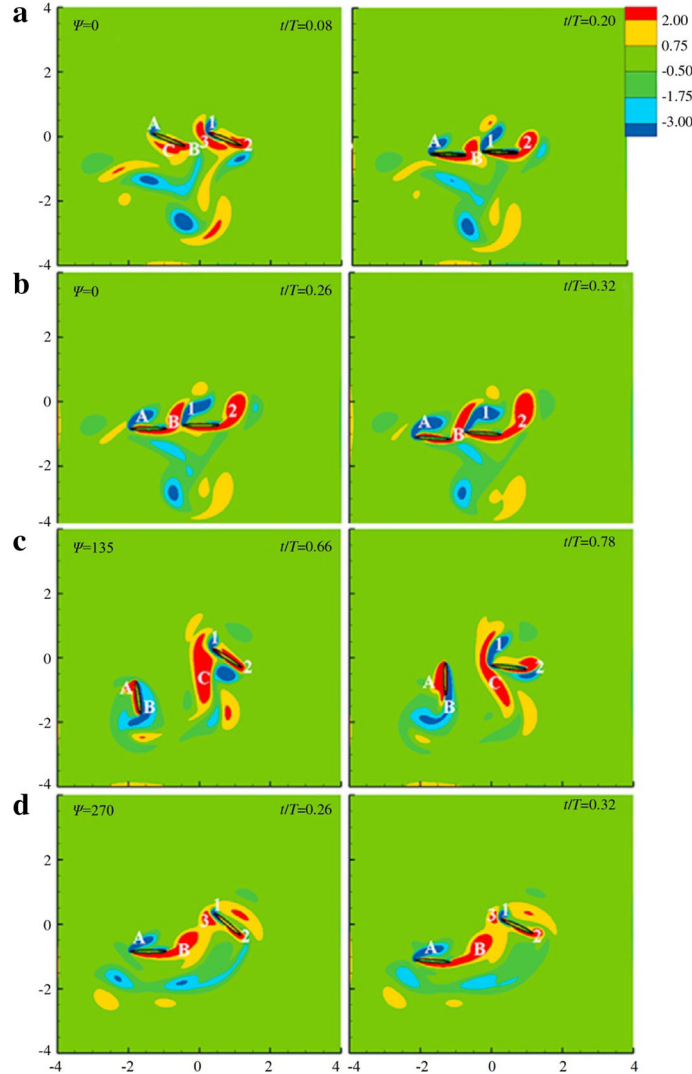


**Fig. 16** Contours of vorticity around the flapping wings at the instants near the lift peaks of **a** the hindwing with a phase angle of  $\psi = 0^\circ$ , **b** the forewing with  $\psi = 0^\circ$ , **c** the hindwing with  $\psi = 135^\circ$ , and **d** the forewing with  $\psi = 270^\circ$  [63]

only significantly influences the lift performance under certain kinematic conditions and it affects more on the aerodynamic performance of the hindwing than the forewing. One result obtained by Xie et al. is demonstrated in Fig. 16. Vorticity contours around the flapping wings in Fig. 16 are at the instants when the lift coefficients of forewing or hindwing reach the peak values in the time histories. It has been found that the vortex interactions between forewing and hindwing can be beneficial to the enhancement of the lift force of the wings, but the aerodynamic benefit of wing–wing interaction is affected by the relative phase difference  $\psi$  between forewing and hindwing stroke cycles.

However, Russell [21] pointed out that generally, 2D numerical simulations are sufficient to provide accurate information about the flapping flight mechanism of the dragonfly, but a certain level of bias still exists. Namely, the value of the 2D numerical predicted force is greater than the experimental value at large angles of attack, whereas it becomes smaller than the experimental measurement at small angles of attack. Therefore, more and more researchers have tried to reveal the aerodynamics of dragonfly flight using a complete 3D model of the dragonfly. Wang and Sun [42] have performed 3D simulations of the flapping motions of the fore- and hindwings. Figures 17 and 18, respectively, display spanwise component of vorticity at various time during one stroke cycle for forewing and hindwing of dragonfly in hovering flight. In Figs. 17 and 18, the forewing–hindwing phase angle difference is  $180^\circ$ . In addition, the red solid lines represent the wing, solid and broken black lines indicate positive and negative vorticity, and  $\tau_1 \sim \tau_6$  indicate various non-dimensional times during

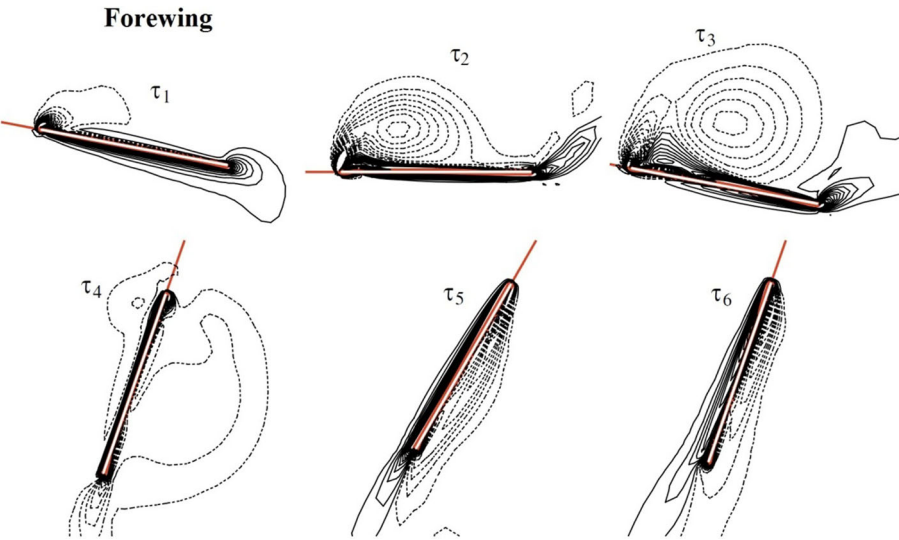


**Fig. 17** Plot of spanwise component of vorticity at half-wing length at various times in one stroke cycle for the forewing [42] (difference in phase angle between the hindwing and forewing  $\psi = 180^\circ$ ; geometric angles of attack in downstroke  $\alpha_d = 52^\circ$  and upstroke  $\alpha_u = 8^\circ$ ; non-dimensional time  $\tau$ )

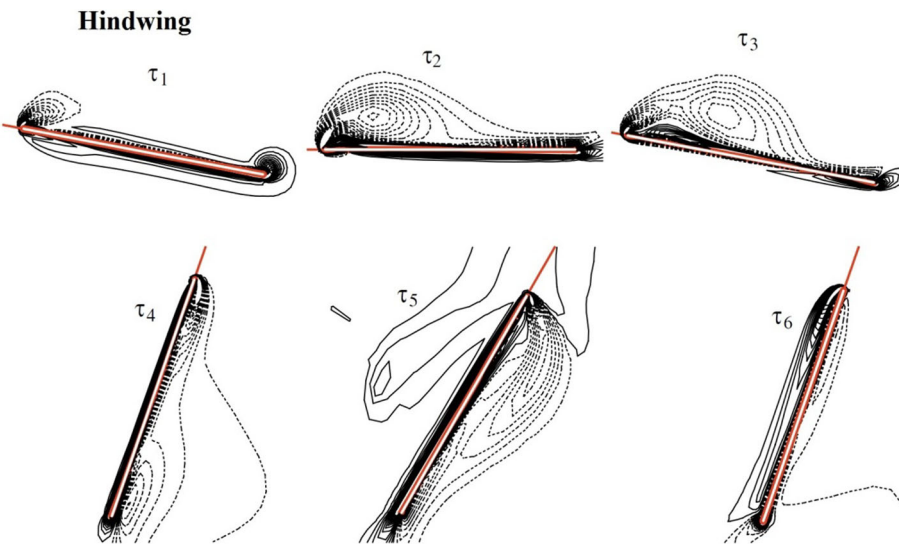


**Fig. 18** Plot of spanwise component of vorticity at half-wing length at various times in one stroke cycle for the hindwing [42] (difference in phase angle between the hindwing and forewing  $\psi = 180^\circ$ ; geometric angles of attack in downstroke  $\alpha_d = 52^\circ$  and upstroke  $\alpha_u = 8^\circ$ ; non-dimensional time  $\tau$ )

one stroke cycle. During both the fore- and hindwing downstrokes, the formation, growth and shedding of the LEV as well as the complex flow recirculation at the trailing edge induced by the LEV can be seen. However, during upstrokes of fore- and hindwing, the flow remains attached all the way to the trailing edge of both the forewing and the hindwing, indicating that the effective angle of attack of both wings is very close to  $0^\circ$ . These results are substantially different from those observed from the 2D simulations in which upstroke acts as the reverse motion of a downstroke, and no such significant difference is expected. In addition, it can be seen from Figs. 17 and 18 that the flow around the hindwing during its upstroke is clearly affected by the motion of the forewing, like the vorticity contour at time instant  $\tau_5$ . During the downstroke, the size of LEV of the hindwing is obviously smaller than that of the forewing, such as the vorticity contour plots at time instant  $\tau_2$  and  $\tau_3$ .

Sun and Lan [65] computationally analyzed aerodynamic force characteristics of flapping wings in hovering flight. Their result of the total vertical force coefficient which is the sum of vertical force coefficient of the fore- and hindwings is presented in Fig. 19. Sun and Lan found that two peaks of the total vertical force coefficient,

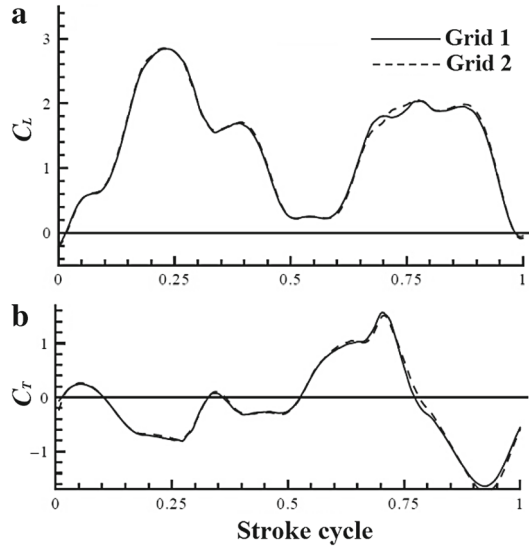


**Fig. 19** Variation of total vertical force coefficient ( $C_L$ ) and total thrust coefficient ( $C_T$ ) with time in one stroke cycle [65]

respectively, corresponding to the forewing downstroke and the hindwing stroke appeared alternatively during the first half and the second half of the dragonfly's wing-stroke cycle. According to the data presented in Fig. 19, the averaged total vertical force coefficient over one flapping cycle is approximately equal to the dragonfly's weight and the time average over one cycle of the total thrust coefficient is nearly zero. As a result, the dragonfly can maintain a balanced, hovering flight. The aerodynamic forces acting on the forewing and hindwing were also analyzed separately by Sun and Lan, and their results are presented in Fig. 20. For both forewing and hindwing, it is noted that the vertical force coefficient peaks during the wings' downstroke and becomes very small when the wings are pulled up (the upstroke). Sun and Lan suggested that the unsteady flow effect and the interaction between the two wings are the possible reasons that might be responsible for the generation of large vertical force coefficient. By comparing to a single wing, they also indicated that although the interaction between the two wings is not very strong in hovering flight, it intends to decrease the vertical force generation.

Sun and Tang [66] presented the equations to calculate the aerodynamic power required by dragonfly for flight, and they divided it into two parts: one  $C_{Q,a,t}$ , which is due to the aerodynamic torque for translation, is calculated using Eq. (11); and another one  $C_{Q,r,t}$  is due to the aerodynamic torque for rotation and calculated using Eq. (12).

$$C_{Q,a,t} = \frac{Q_{a,t}}{0.5\rho V_\infty^2 Sc} \quad (11)$$

$$C_{Q,a,r} = \frac{Q_{r,t}}{0.5\rho V_\infty^2 Sc} \quad (12)$$

where  $Q_{a,t}$  and  $Q_{a,r}$  are the aerodynamic torque around the axis of azimuthal rotation and the axis of pitching rotation, respectively.  $S$  denotes the area of one wing.  $c$  is the mean chord length.

The aerodynamic power coefficient is defined as:

$$C_{P,a} = \frac{P_a}{0.5\rho V_\infty^3 S} \quad (13)$$

$C_{P,a}$  then can be calculated as below:

$$C_{P,a} = C_{Q,a,t}\dot{\phi}^+ + C_{Q,r,t}\dot{\alpha}^+ \quad (14)$$

where  $\dot{\phi}^+$  is the non-dimensional angular velocity of azimuthal rotation and  $\dot{\alpha}^+$  is the non-dimensional angular velocity of pitching rotation.

The aerodynamic power requirements of dragonfly hovering were then assessed by Sun and Lan [65] and are displayed in Fig. 21. Their results show that no matter forewing or hindwing, the maximum power

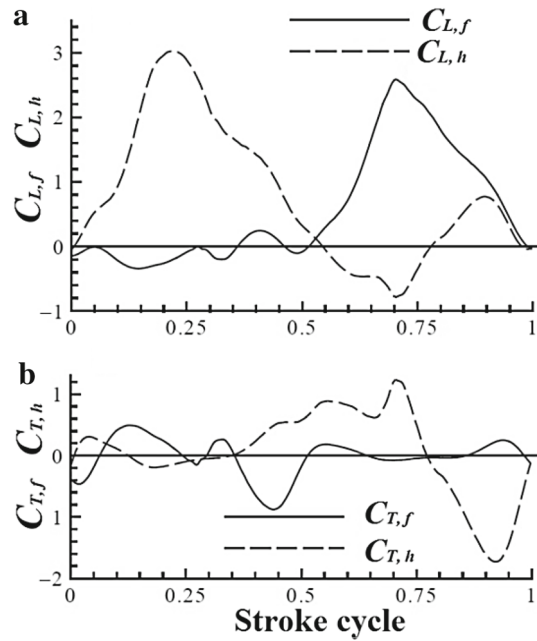


**Fig. 20** The time variation of vertical force coefficients of forewing ( $C_{L,f}$ ) and hindwing ( $C_{L,h}$ ) as well as thrust coefficients of the forewing ( $C_{T,f}$ ) and the hindwing ( $C_{T,h}$ ) in one cycle [65]

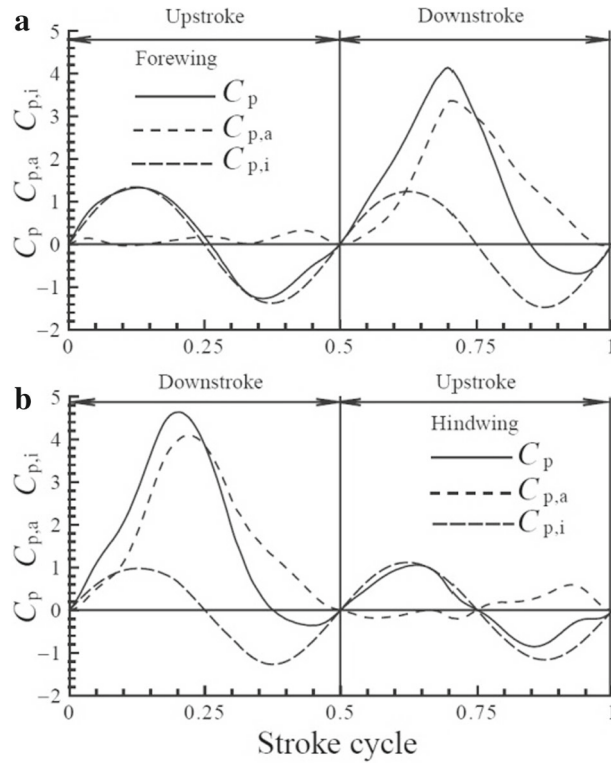


**Fig. 21** Time variation of power coefficients of forewing (a) and hindwing (b) in one cycle.  $C_p$ , power coefficient;  $C_{p,a}$ , coefficient of power due to aerodynamic force;  $C_{p,i}$ , coefficient of power due to inertial force [65]

consumption is required during both the upstroke and downstroke of the wings. Besides, the power requirement of downstroke is apparently greater than that of upstroke. This is reasonable since the power required for the downstroke is mainly used to produce the vertical force and the power requirement for the upstroke that is

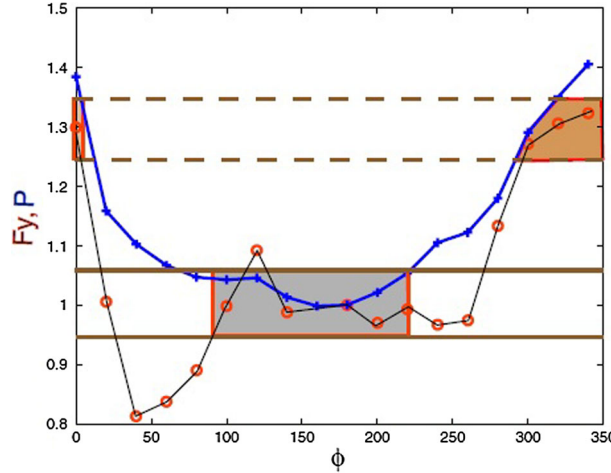


**Fig. 22** Time-averaged vertical force  $F_y$  (black line with circle marker) and power  $P$  (blue line with plus sign marker) [22]. (Color figure online)

needed to overcome the aerodynamic drag is relatively small due to nearly 0 degree angle of attack. It is observed that during the upstroke of both forewing and hindwing, main power requirement is from inertial power  $C_{p,i}$ , but aerodynamic power  $C_{p,a}$  becomes the dominant source of power during the downstroke of the wings. When hovering, it seems that dragonfly can also harness energy in the air instead of merely consuming power, because of the presence of negative power coefficient. This phenomenon possibly results from the rotation of the wings near the end of their upstroke.

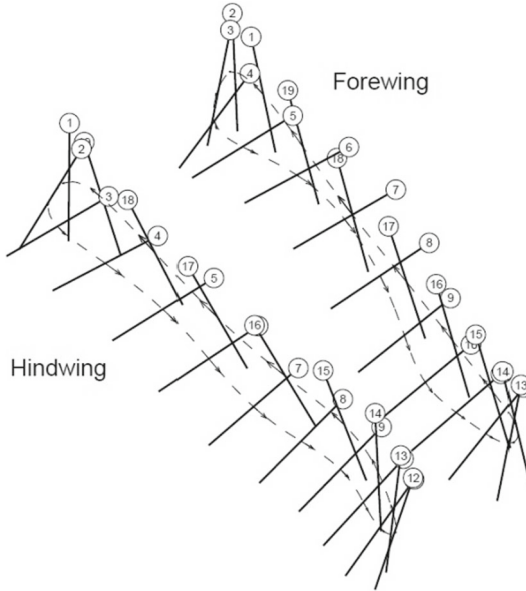
Furthermore, some experimental researchers have noticed that the phase angle between the forewing and the hindwing is not always  $180^\circ$  in hovering flight of dragonfly. As shown in Fig. 22, Russell et al. at Cornell University [22] found that when dragonflies hover, the mean vertical force ( $F_y$  in Fig. 22) and the mean output power ( $P$  in Fig. 22) of the dragonflies corresponding to the phase angles within a certain range (the light gray area shown in Fig. 22) remain roughly constant, and therefore, this result may be able to explain these experimental findings.

### 3.3 Accelerated flight

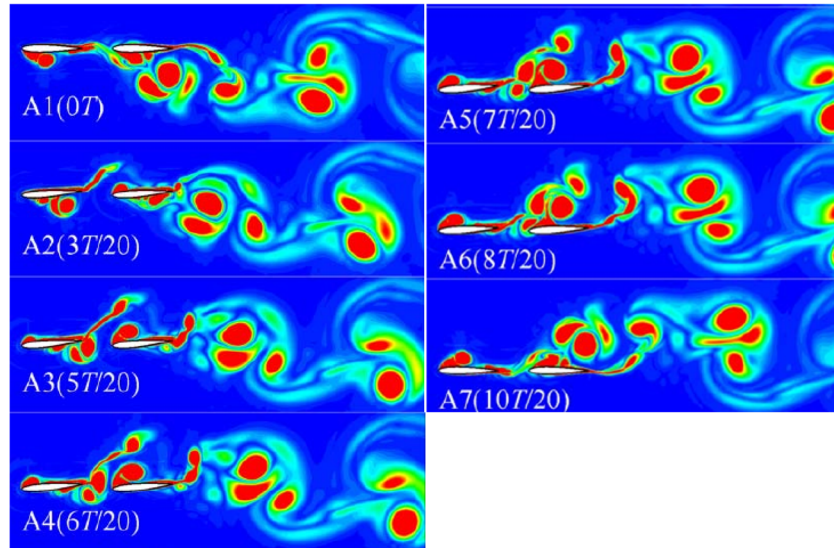
In acceleration, dragonflies can switch to in-phase wing beats with  $0^\circ$  phase difference between their forewings and hindwings [23]. As a result, enough lift and thrust can be generated to allow dragonflies to accelerate for brief intervals to speeds of up to 13.4 m/s [67]. However, as it requires a significant amount of power and only last a very short period of time [19], acceleration appears to be a kind of flight behavior that is less efficient. Therefore, dragonflies accelerate during their takeoff or prey pursuit when requirements of high lift and thrust forces are imperative. As the small relative motion of two adjacent sets of wings occurred, acceleration mode is relatively easy to be understood by dragonfly researchers.

Figure 23 shows 2D schematics of the relative position between the forewing and the hindwing of an accelerating dragonfly [21]. Except at the end of the upstroke and downstroke of the flapping circle, it is observed that the forewing and hindwing are positioned nearly in parallel, that is, the relative phase difference between fore- and hindwings is about  $0^\circ$  during one period of stroke. The forewing and hindwing are not moving in parallel next to each other due to wings rotational motion at the end of upstroke and downstroke.

Xiao [54] still used the model shown in Fig. 14 to examine the vorticity fields around the flapping wings as the dragonfly accelerates. In this case, the phase difference between fore- and hindwings in his numerical model is approximately zero and his results are presented in Fig. 24. By comparing to Fig. 15, it can be seen that the simulated flow field around the forewing looks like that shown in dragonfly's hovering flight. During the downstroke of the hindwing, a leading-edge vortex is created on its upper surface (as shown in A1 of Fig. 24). Due to the influence of upward flow induced by its previous upstroke motion, the angle of attack of hindwing (angle between the chord of the wing and the relative wind) is greater than that of forewing, and as a result, the LEV formed on the upper surface of the hindwing grows rapidly in both size and strength (as shown in A2–A4 of Fig. 24). Near the end of the downstroke, the LEV is eventually shed from the hindwing under



**Fig. 23** 2D schematics of the relative position between the hindwing and the forewing of a dragonfly in acceleration mode: The leading edge of each wing is marked with a circle, the number inside the circle is a time index, the dashed line represents the path of the center of the wing, and the arrows on the dashed line indicated velocity [21]



**Fig. 24** 2D vorticity contours around the flapping wings of a dragonfly in acceleration mode [54]

the influence of the wake flow of forewing (as shown in A5–A7 of Fig. 24). His results therefore confirm that high flight forces have been correlated with in-phase flapping of fore- and hindwings, i.e., both wings flap in synchronization.

Xiao [54] further quantitatively analyzed the vertical force, drag and power production required by a dragonfly to accelerate to top speed in a fraction of a second, and his simulation results are presented in Fig. 25. It is found that the peak values of both the total lift force and drag produced by accelerating (the red line) are much higher than those generated by a dragonfly in hovering flight (the green line). However, the flight forces by wings flapping in phase generally appear to be less stable than those generated by out-of-phase wingbeats in hover: Aerodynamic forces reach their peak values in the first half of the cycle due to the downstroke motion of both wings and the lift force and then rapidly decrease because of the shedding of the leading-edge vortices. A second peak value of drag force is also seen in the second half of the cycle, and this could be confusing as

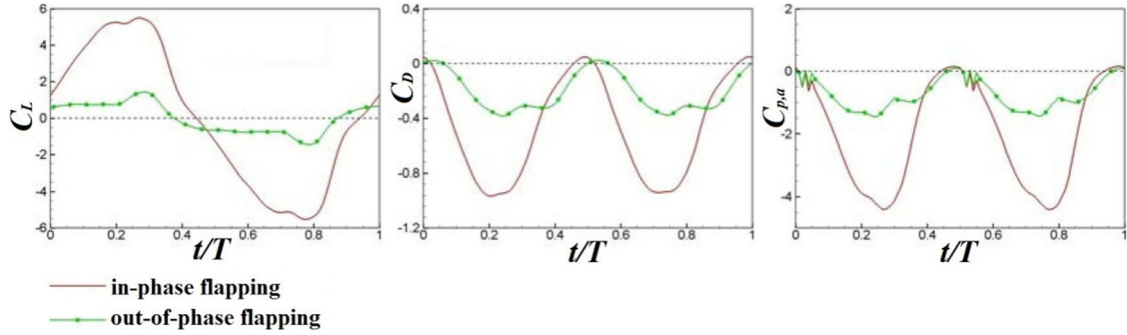


**Fig. 25** Comparison of the lift force, drag force and aerodynamic power requirement between in-phase and out-of-phase flapping of a dragonfly [54]

experimental studies suggest the angle of attack of the wings during the upstroke is relatively small, and thus, the generated aerodynamic drag should also be much smaller. In addition, a comparison between the power output obtained from in-phase and out-of-phase flapping shows that the in- phase flapping wings are able to generate higher net thrust at the expense of a massive increase in aerodynamic power requirements.

### 3.4 Forward flight

Forward flight, also called cruising flight, is most commonly observed in dragonflies which can reach forward flight speed up to 100 body lengths per second. In straight forward flight, dragonfly's hindwing leads forewing with a phase shift of 54°–100° [40] and thus produces higher thrust and efficiency in comparison with that obtained with a single flapping wing. Thus, the forward flight of a dragonfly can be regarded as a type of flight mode between acceleration and hovering.

According to Fig. 26 which shows the relative position between the forewing and the hindwing, it can be seen that the phase difference between the two wings is nearly 90° out-of-phase for a dragonfly in forward flight. The angle of attack of dragonfly's wings becomes progressively smaller during the downstroke, whereas it becomes larger in the course of the upstroke in forward flight mode.

The kinematic parameters applied by the dragonfly in the forward flight posture were measured by Wang et al. who developed a method based on a projected comb-fringe technique [40]. According to their measurement data illustrated in Fig. 27a, the dragonfly travels along an axon ( $Y$  axis) in only one direction during forward flight. A process of increasing the pitch angle of the dragonfly can be clearly seen in Fig. 27b, while the roll and yaw angles are kept at almost constant values over time. Moreover, there are only angular velocity and acceleration of the pitching motion, while the angular velocity and acceleration of the roll or yaw motion are almost zero, as shown in Fig. 27c, d.

Wang and Sun used the following equations to describe the wing kinematics of dragonflies in forward flight [42]. The flapping angle of dragonfly wing is expressed as below:

$$\varphi = \Phi \cos(\omega t + \gamma_d) \quad (15)$$

where  $\omega = 2\pi f$ ,  $f$  is the flapping frequency.

They assumed that the wing rotated around the axis located at 1/4 chord length and the corresponding equation can be presented as follows:

$$\dot{\vartheta}_{(\tau)} = 0.5\dot{\vartheta}_0 \{1 - \cos[2\pi(\tau - \tau_{au})/\Delta\tau_R]\}, \quad \tau_d \leq \tau \leq \tau_d + \Delta\tau_R \quad (16)$$

$$\dot{\vartheta} = (\pi - \alpha_u - \alpha_d)/(\Delta\tau_R T) \quad (17)$$

Rotating movement of the wing during downstroke and upstroke occurs at time  $\tau_d$  and  $\tau_u$ , respectively.  $\Delta\tau_R$  is the time interval over which the rotation lasts.

From their simulation results displayed in Fig. 28, it is noted that in forward flight, the aerodynamic forces produced by the movement of wing flapping are not strongly relied on the existence of a large LEV like hovering flight (Fig. 28a), but on a thick vortex layer extending over the whole wing surface (Fig. 28b, c). With the increase in forward speed, it looks like the vortex layer is depressed much closer to the surface of the wing,

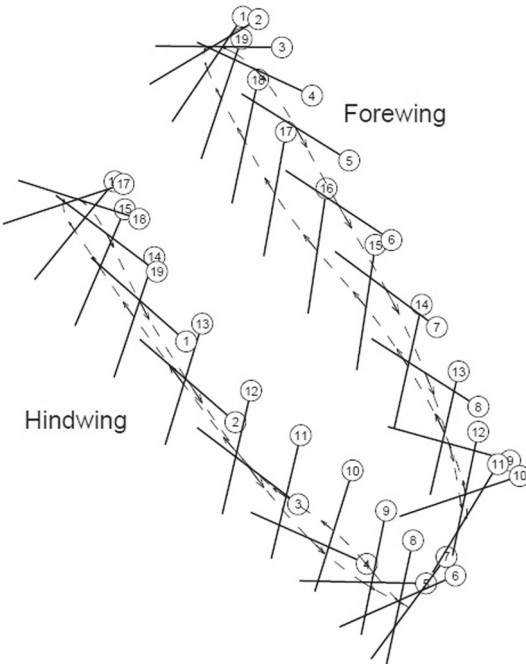


**Fig. 26** 2D schematics of the relative position between the hindwing and the forewing of a dragonfly in forward flight: The leading edge of each wing is marked with a *circle*, the *number inside the circle* is a time index, the dashed line represents the path of the center of the wing, and the arrows on the dashed line indicated velocity [21]

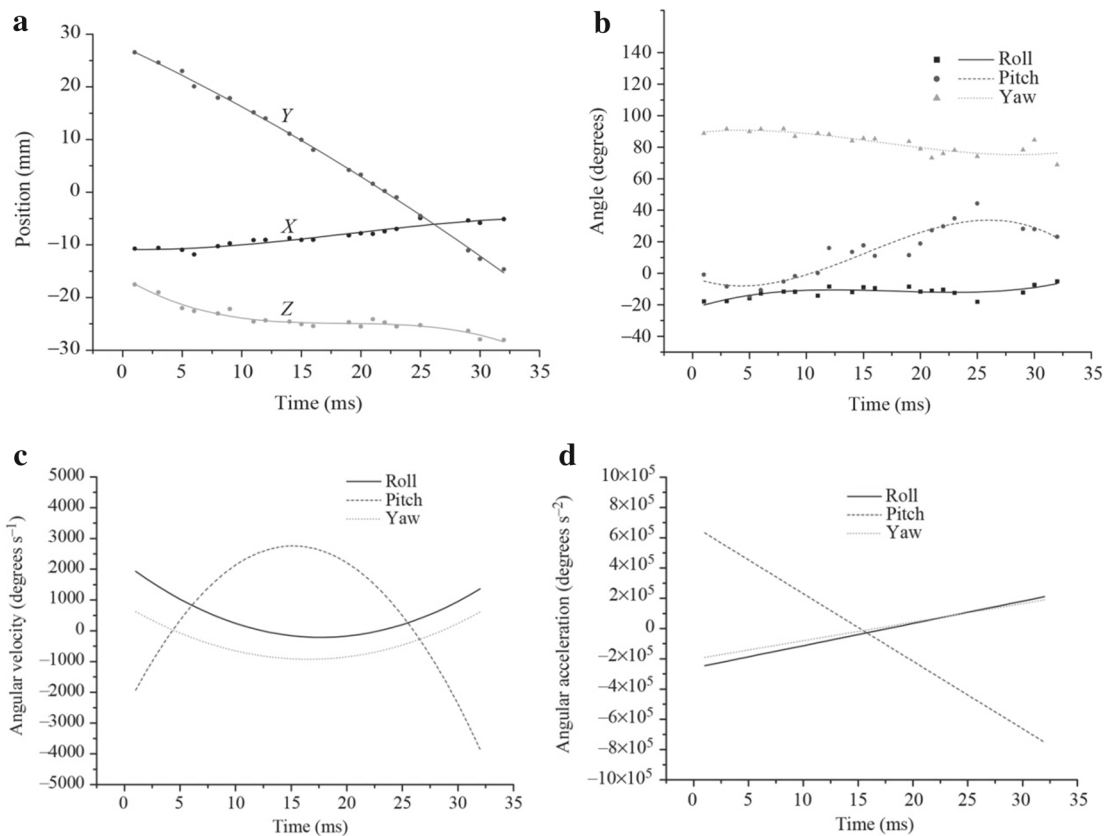


**Fig. 27** The measured flight trajectory, velocity and acceleration during forward flight [40]

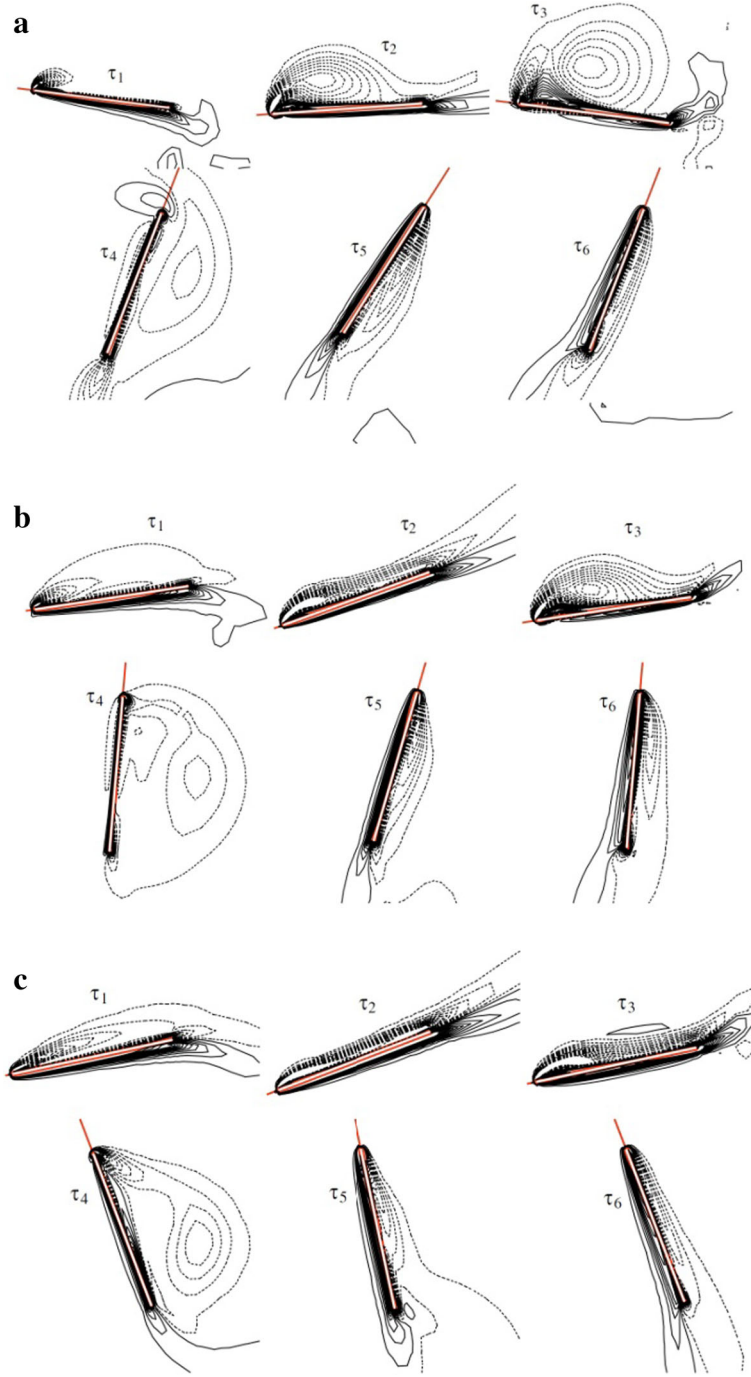


**Fig. 28** Plot of spanwise component of vorticity at half-wing length at various time in a stroke cycle for the forewing, at  $\psi = 60^\circ$ , **a**  $J = 0.0$  ( $\alpha_d = 48^\circ$  and  $\alpha_u = 5.5^\circ$ ); **b**  $J = 0.3$  ( $\alpha_d = 32^\circ$  and  $\alpha_u = 21.8^\circ$ ); **c**  $J = 0.6$  ( $\alpha_d = 31^\circ$  and  $\alpha_u = 50^\circ$ ). *Solid* and *broken* lines indicate positive and negative vorticity, respectively; the magnitude of non-dimensional vorticity at the outer contour is 1 and the contour internal is 3.  $\psi$ , difference in phase angle between the hindwing and forewing;  $J$ , advance ratio;  $\alpha_d$  and  $\alpha_u$ , geometric angles of attack in the down- and upstrokes, respectively;  $\tau$ , non-dimensional time [42]

indicating that flow around the forewing becomes more attached (Fig. 28c). Similar results were also obtained for the hindwing. As illustrated in Fig. 29, it assumes that aerodynamic forces produced by a dragonfly in flight are closely associated with the incoming flow and the flapping velocity of the wing. When the forward flight speed is low, the formation of large-scale vortex structures, which originate from the wing leading edge,

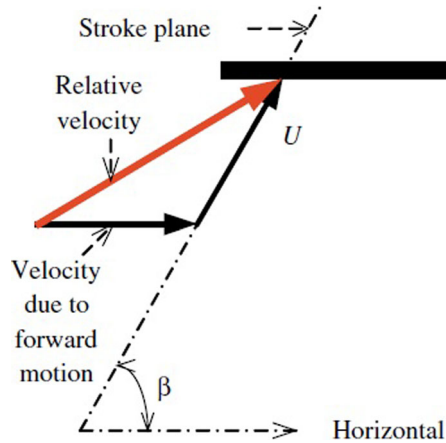


**Fig. 29** Diagram of wing cross section with velocity triangle.  $\beta$ , stroke plane angle;  $r_2$ , radius of the second moment of wing area;  $U$ , velocity due to flapping [42]

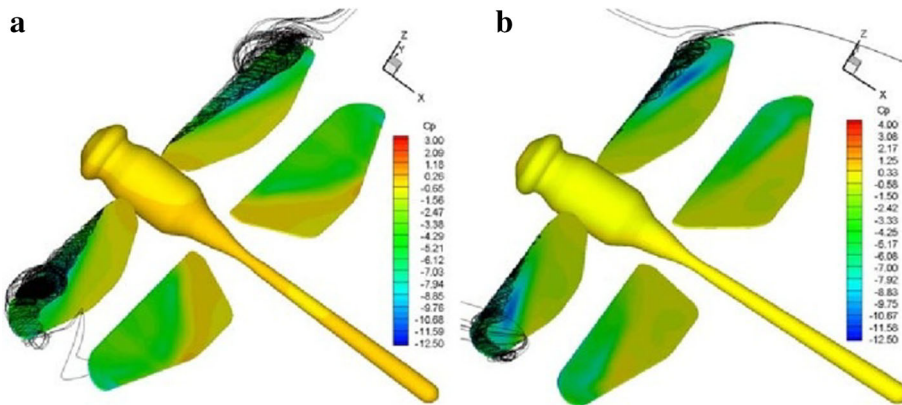


**Fig. 30** The pressure distribution and streamlines passing along the upper surface of dragonfly's wings: **a** hovering flight; **b** forward flight.  $J$  advance ratio;  $\Psi$  difference in phase angle between the hindwing and forewing [54]

is imperative in order to attain much higher lift values that can sustain the weight of the dragonfly. However, at high forward flight speed, high aerodynamic forces are more likely to be associated with the attached-flow regime that covers much of the wing surface. In addition, as the forward speed increases, the angle of attack of the wing during upstroke is gradually decreased, while the angle of attack of the wing during downstroke is continuously increased. This is a tactic adopted by the dragonfly to maintain the net collective result of a steady force acting on it.

Xiao [54] created full-body 3D simulations of a four-winged dragonfly in free flight. His results shown in Fig. 30 also suggest that compared to the hovering flight, the leading-edge vortex formed in forward flight is much smaller and attached flow over the wing is dominant.

Wang and Sun's quantitative assessments of aerodynamic forces generated in forward flight are given in Fig. 31. Different from aerodynamic forces generated during hovering flight, the vertical force coefficient  $C_V$  on the dragonfly wings in forward flight has only one peak value during one complete flapping cycle and its value is greater than that produced in hovering flight. As the forward speed increases, the peak value for the vertical force coefficient also increases. In addition, the average thrust force  $C_T$  on the complete set of wings, over a complete cycle of wing movements, cannot be canceled out and has a positive value that is used to propel the dragonfly forward.

The influence of interaction between fore- and hindwings on aerodynamic forces generation was also analyzed and is presented in Fig. 32. According to Wang and Sun's results, it can be found that at most of time, the inference between the fore- and hindwings is not conducive to the increase of vertical force coefficient and thrust coefficient. If considering the average value over one cycle, the interaction between the wings actually leads to a 14.3% reduction in vertical force during hovering flight ( $J = 0$ ), a 7.5% reduction in vertical force

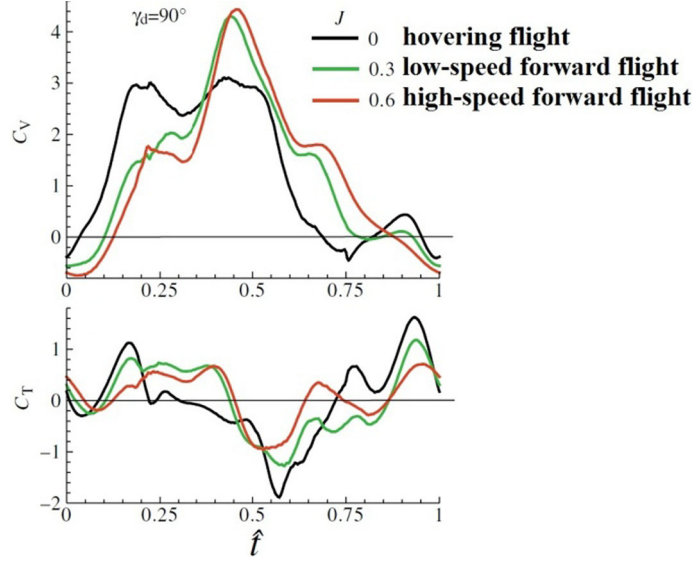


**Fig. 31** The time variation of vertical force coefficient  $C_V$  and thrust force coefficient  $C_T$  for hovering and forward flight [42]

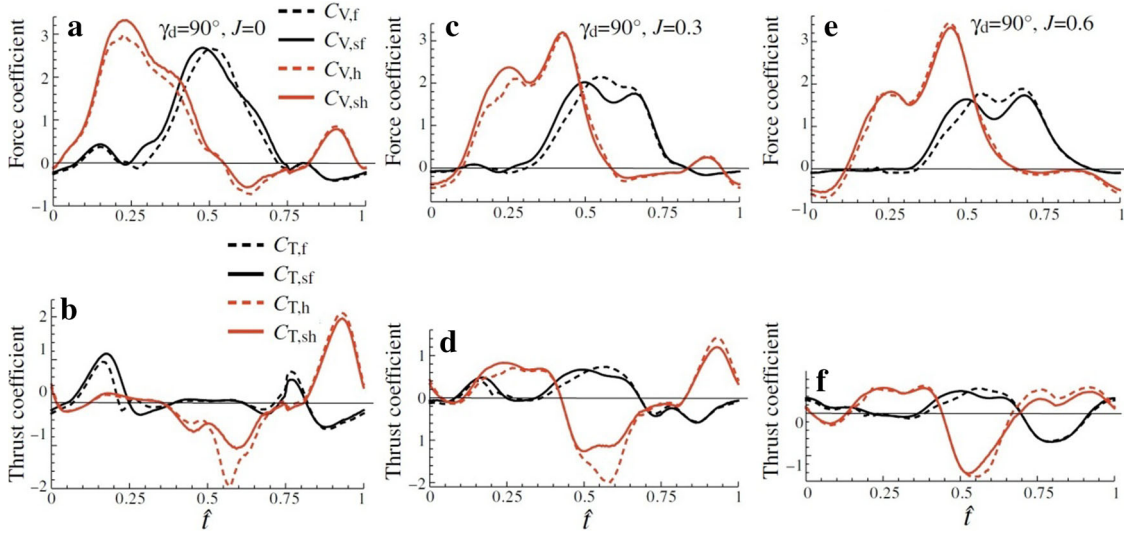


**Fig. 32** Time variation of vertical force coefficients of forewing ( $C_{V,f}$ ), single forewing ( $C_{V,sf}$ ), hindwing ( $C_{V,h}$ ) and single hindwing ( $C_{V,sh}$ ) and thrust coefficients of the forewing ( $C_{T,f}$ ), single forewing ( $C_{T,sf}$ ), hindwing ( $C_{T,h}$ ) and single hindwing ( $C_{T,sh}$ ) in one cycle; **a, b**  $\gamma_d = 90^\circ$ ,  $J = 0$ ; **c, d**  $\gamma_d = 90^\circ$ ,  $J = 0.3$ ; **e, f**  $\gamma_d = 90^\circ$ ,  $J = 0.6$ .  $\gamma_d$ , difference in phase angle between the hindwing and forewing;  $J$ , advance ratio;  $\hat{t}$ , non-dimensional time [42]

during forward motion with a medium forward speed ( $J = 0.3$ ), and a 1.6% reduction in vertical force for high-speed forward flight ( $J = 0.6$ ).

### 3.5 Free-flight turning maneuvers of dragonflies

So far, fully understanding of free-flight turn maneuver of dragonflies can still be challenging, and current studies on this flight behavior of dragonflies are mostly based on images captured by high-speed photography. Videos of dragonfly flight show that when the dragonfly executes a fast turn, its wings flap asymmetrically and one wing moves independently of the other [40, 68]. Moreover, research on the dynamics of turning maneuvers in dragonflies via quantitative measurements or accurate numerical simulations is still limited.

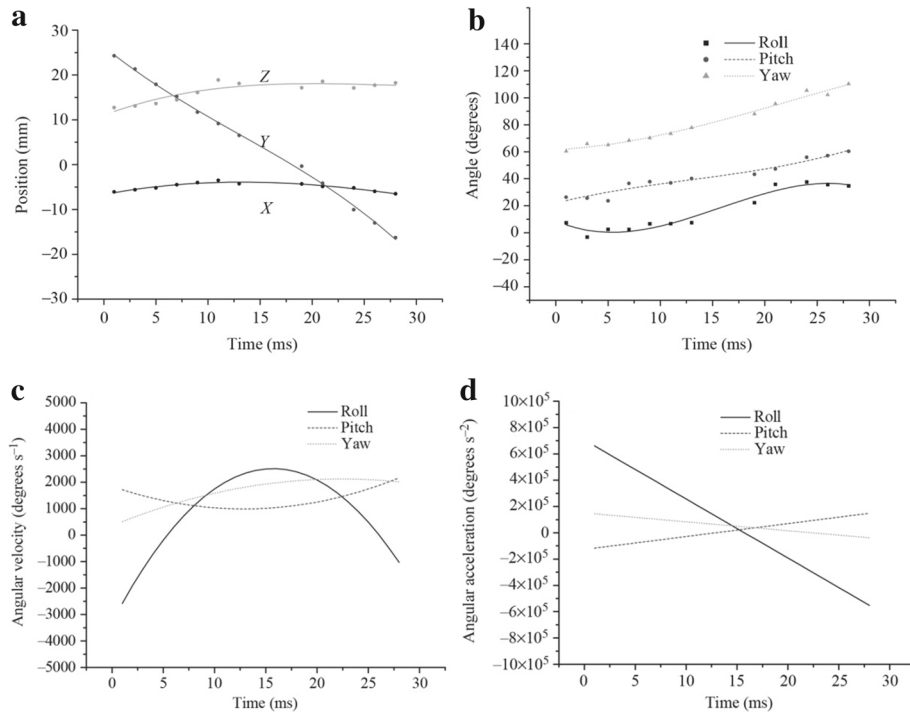


**Fig. 33** The measured flight trajectory, velocity and acceleration of turning maneuvers in dragonfly [40]

As one of the most sophisticated flying machines, the dragonfly can execute a proper turn at high speed and the video recordings show that it can turn 180° in only three wingbeats. However, in all flight modes studied so far, turning maneuvers of dragonflies are still an archetype of complex flight behaviors. There has been very little research reported on the turning maneuvers of dragonflies due to the complexity of many issues involved such as the exact determination of the inclined angle of dragonfly body and the relative arrangement of the forewing and hindwing. Current studies are heavily relied on observations, and measurements taken during experiments as the accurate numerical simulation of dragonflies turning in flight are still a challenging task. According to the experimental results obtained by Wang et al. [40], the data of angular velocity of free-flying dragonfly as it turns in midair show an asymmetric distribution over time (see Fig. 33c). This is different from the results presented in Fig. 27c in which the time variations in angular velocity present a nearly right-left symmetric distribution. In addition to the variation of pitch angle shown in Fig. 33b, both the roll and yaw angles grow at a roughly same rate over time during turning maneuvers, suggesting that the tested dragonfly was making a right turn with the body inclined right and the head raised up.

Wang et al. further investigated the difference in flapping angle, torsional angle and camber deformation between forward flight and turning maneuvers for the tested dragonflies. As seen in Fig. 34, dragonfly changes the movement and morphological parameters of its individual forewing and hindwing during the flapping motions in order to meet the performance requirements of different flight.

Much more research is needed on turning maneuvers in dragonflies. In this way, the results can be enough to corroborate each other and discover the aerodynamic properties bodies and wings.

## 4 Factors affecting aerodynamics of dragonfly flight

### 4.1 Influence of wing flapping trajectories

The wing flapping trajectories of a dragonfly studied in most of the above studies were assumed to be a reciprocating motion along a stroke plane inclined at a certain angle with respect to horizontal. However, this may not be an exact simplification according to Xu et al.'s work. As depicted in Fig. 35, Xu et al. believed that the ellipse, the simple figure-eight and even the double-figure-eight flapping trajectory were closer to the functional behavior of the dragonfly wing. It should be noted that the wing flapping trajectory herein

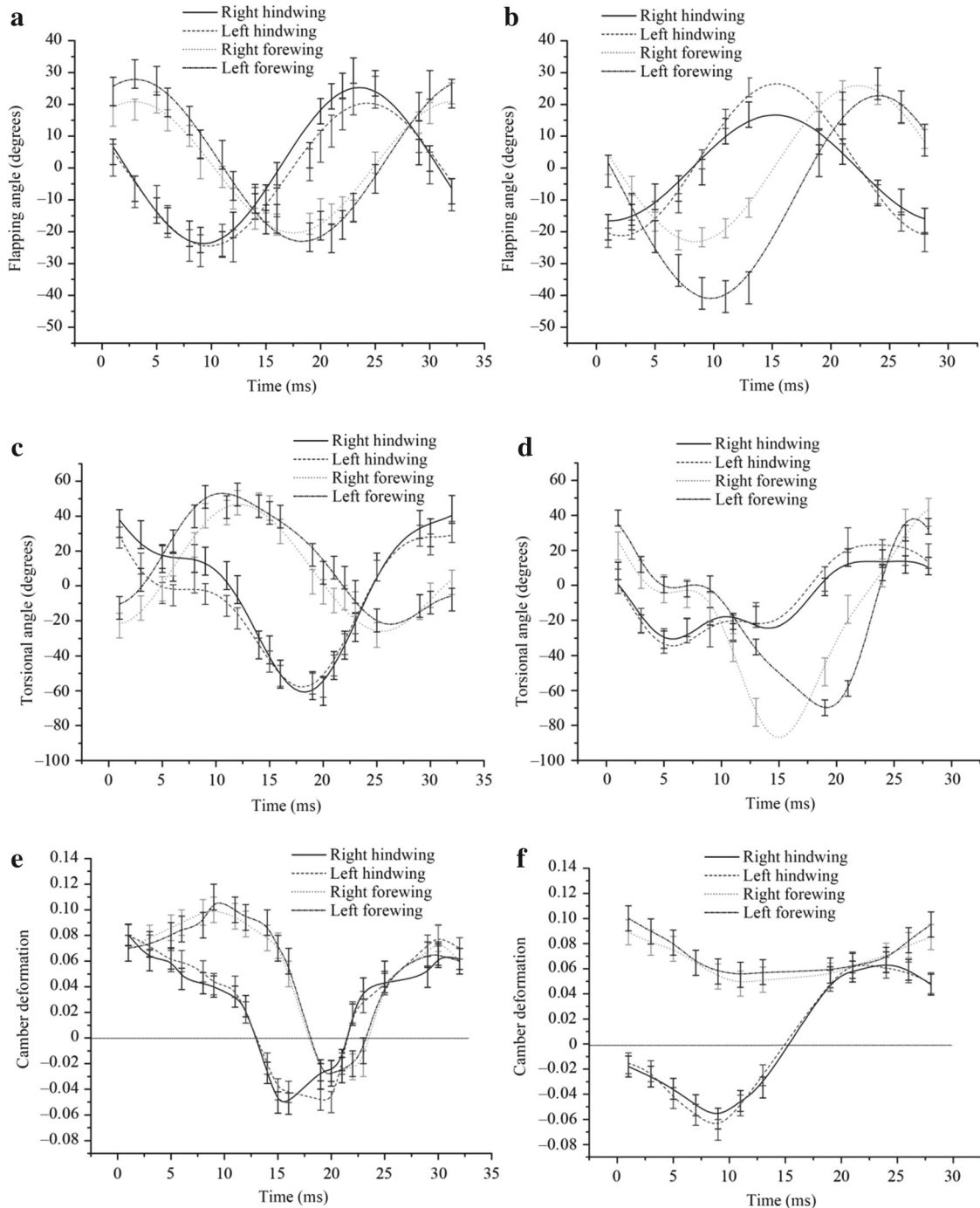


**Fig. 34** Wing kinematics for two flight behaviors: **a, c, e** for forward flight; **b, d, f** for turning maneuvers. The middle of the error bar is the value of measured data point [40]

is normally recognized as the motion trajectory of the wing's pitch rotation center. However, its location sometimes is different for various researchers, some of whom set it to 1/4 of the chord length back from the wing's leading edge. In Xu's article [69], the pitch axis was at 50% chord and numerical analysis of the aerodynamic characteristics of the wing's flapping motion following different trajectories was conducted.

Table 3 shows the averaged lift and drag forces acting on a single forewing for different flapping trajectories. It can be seen that there exists apparent difference among the three motion trajectories in the aerodynamic force

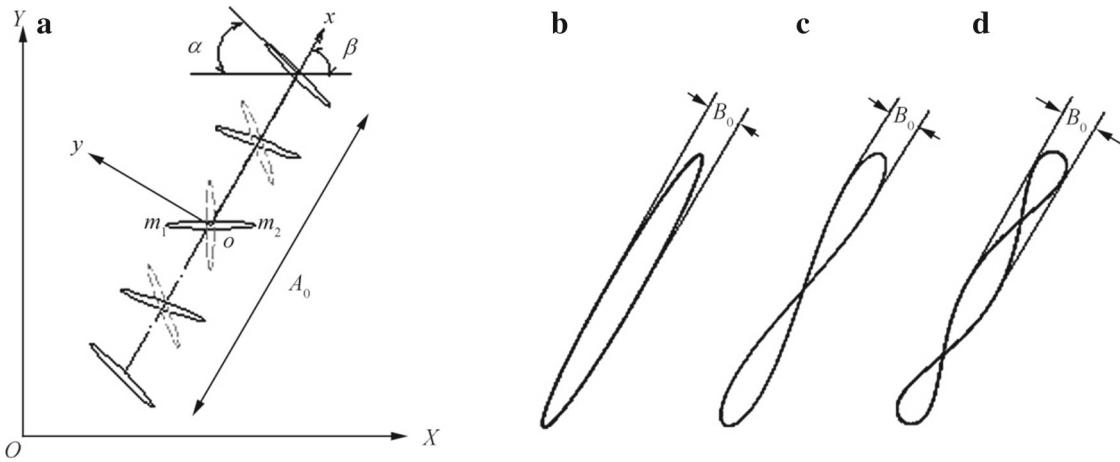


**Fig. 35** Different stroke trajectories in flapping dragonfly wings: **a** the translational flapping trajectory over one flapping cycle. The solid line represents the wing position during downstroke; the dashed line denotes the wing position during upstroke;  $A_0$  is the flapping amplitude;  $B_0$  is the horizontal deviation amplitude;  $\alpha$  is the angle between the wing chord and the horizontal plane; and  $\beta$  is the angle between the wing translational trajectory and the horizontal plane. **b** The ellipse flapping trajectory. **c** The figure-eight-shaped flapping trajectory. **d** The double-figure-eight flapping trajectory [69]

**Table 3** The lift and drag coefficients obtained by using different flapping trajectories [69]

Flapping trajectories of the wing section	Lift ( $C_L$ ) and drag ( $C_D$ ) coefficients	$B_0 = 0$	$B_0 = A_0/10$	$B_0 = A_0/5$
Ellipse	$C_L$	1.46	1.24	0.98
	$C_D$	-0.75	-0.93	-0.99
Figure-eight	$C_L$	1.46	1.76	1.55
	$C_D$	-0.75	-0.88	-0.87
Double-figure-eight	$C_L$	1.46	1.43	1.11
	$C_D$	-0.75	-0.79	-0.70

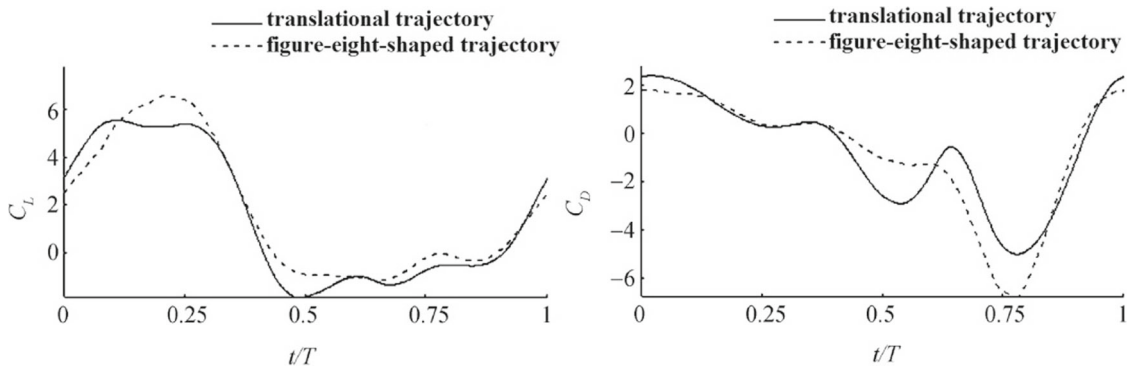


**Fig. 36** Comparison of aerodynamic forces obtained by using the translational trajectory and the figure-eight-shaped trajectory [69]

production and the figure-eight-shaped trajectory appears superior to others in terms of the lift enhancement that it produces. Moreover, difference between aerodynamic forces produced by the wing that follows the different flapping trajectories was compared by Xu et al., and their results are demonstrated in Fig. 36. It can be seen that the time variation of lift and drag forces during one stroke cycle is in fact very similar in both translational and figure-eight-shaped trajectories. This result implies that using translational flapping trajectory may appear qualitatively correct but quantitatively inaccurate.

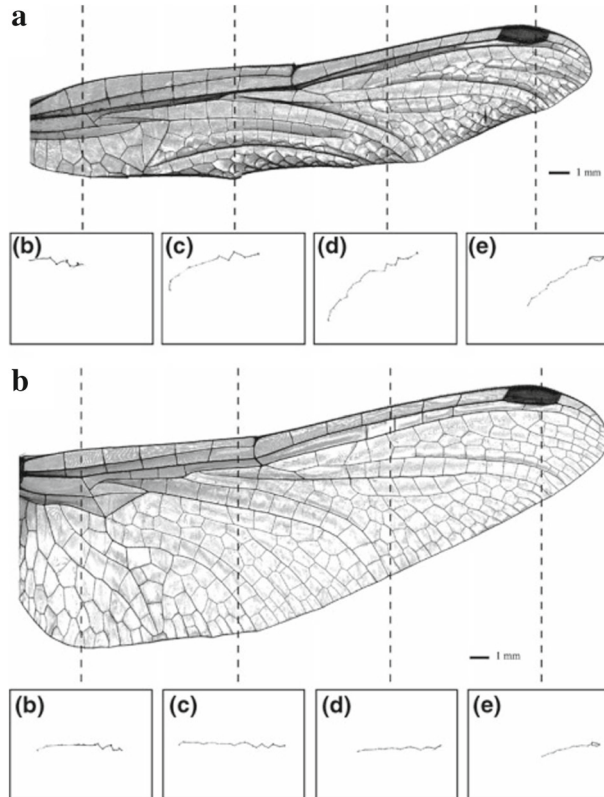


**Fig. 37** Digital reconstruction of the forewing (a) and hindwing of dragonfly (*Sympetrum vulgatum*). Dark areas are thick, light areas are thin (linear scale from dark to light). b–e are the cross-sectional micro-CT images taken at different locations along the wing span [70]

#### 4.2 Influence of wing flexibility

For simplicity, many previous studies assumed that dragonfly wings were rigid structures. However, the actual wings have an inherent flexibility which allows the wings to deform passively under the periodic loading during the dragonfly's flight. Figure 37 is photograph of the real dragonfly's fore- and hindwings. It is revealed that dragonfly wings are composed mainly of veins (stiff member) and membrane (filler material). According to researchers such as Jongerius [70] and Chen [71], the dragonfly's wing looks like a tubular pleated membrane which provides a stiff structure along its spanwise direction and a flexible structure along its chordwise direction. In order to accurately analyze the aerodynamic features of dragonfly wings, they therefore should be treated as flexible structures.

Figure 38 shows the possible strategies of wing morphing during a flapping cycle used by dragonflies in forward flight.

Meng et al. proposed a fluid–structure interactions model of dragonfly flapping flight with flexible wings that employed a 6 degree of freedom [73]. They calculated the time variations of the relative position of the wing's tip within a stroke cycle with respect to the horizontal reference plane. According to their result presented in Fig. 39, it seems that compared to the rigid wing, the flexible wing travels a bit longer distances and there is a time lag between two curves. Therefore, in order to take into account the effect of wing flexibility on the aerodynamic force production, necessary corrections should be applied to the numerical results which are obtained by using a two-degree-of-freedom rigid wing model.

The influence of wing flexibility on the production of aerodynamic forces in flapping flight is further confirmed by Wang et al. who compared the computed flows around rigid forewing of a dragonfly in forward flight to the flows around flexible forewing. As shown in Fig. 40, the leading-edge vortex formed on the top surface of the flexible wing appears larger in size than that of the rigid wing and firmly attaches to the top of the wing. This result is consistent with the results of previous research (e.g., Nakata and Liu [74]) that suggested that flexibility of the wings may stabilize the LEV and result in better aerodynamic performance. In fact, the

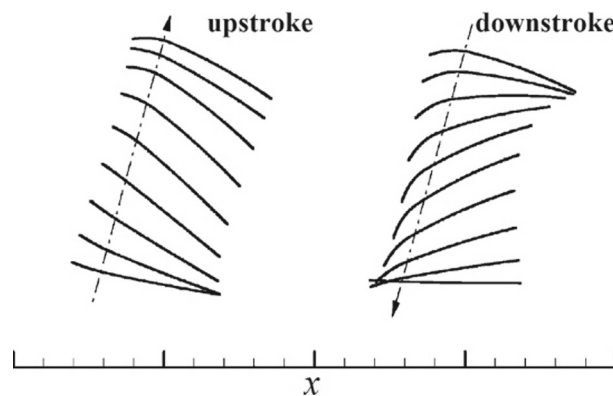


**Fig. 38** Instantaneous wing deformation during a flapping cycle for forward flight [72]

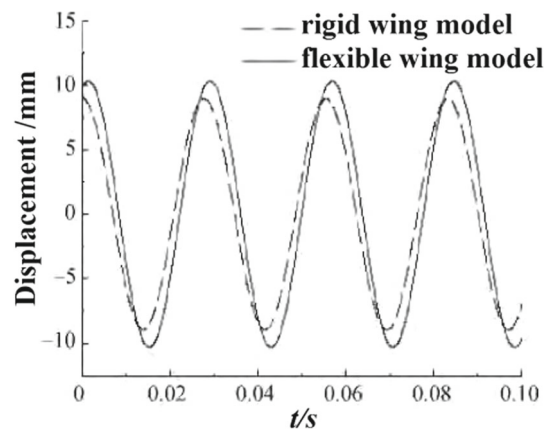


**Fig. 39** Time variation of travel distance for the dragonfly's wing tip [73]

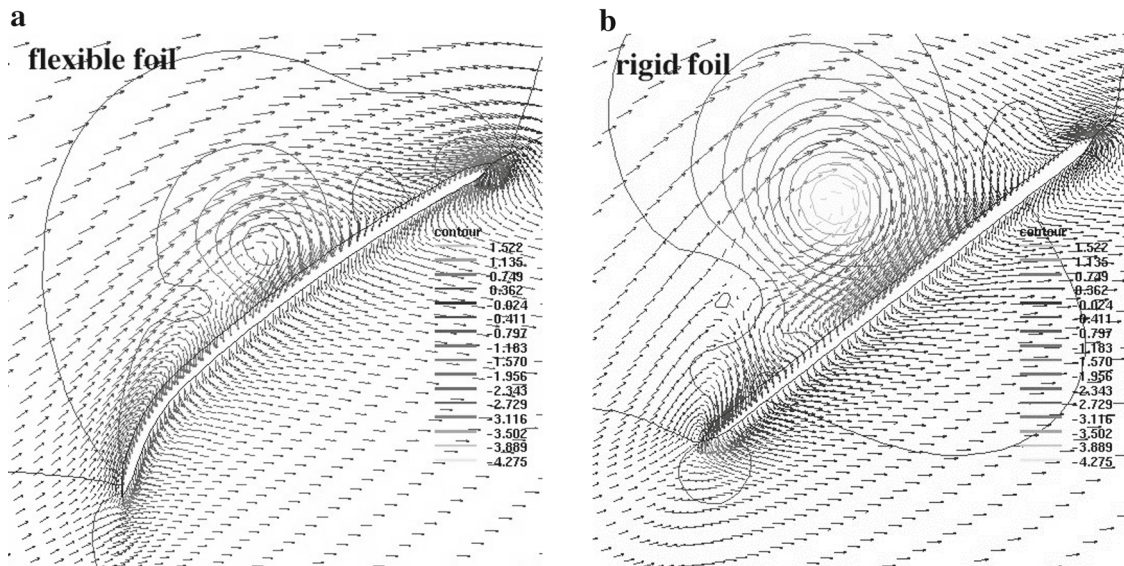


**Fig. 40** Difference in the flow pattern around a flexible wing (a) and a rigid wing at zero flapping angle during downstroke [40]

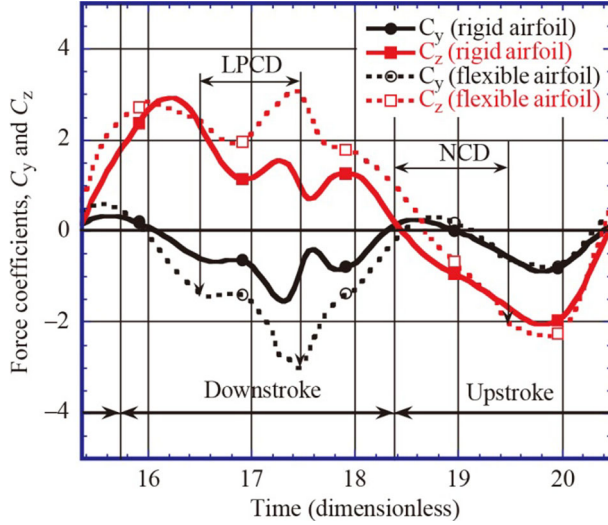


**Fig. 41** Comparison of time-varying force coefficients in a complete beating cycle between the flexible and rigid wings.  $C_y$  is the drag coefficient and its negative value contributes to the force generation of both vertical force and thrust;  $C_z$  is the lift coefficient and its positive value contributes to the vertical force and the drag force. LPCD means larger positive camber deformation; NCD is the negative camber deformation [40]

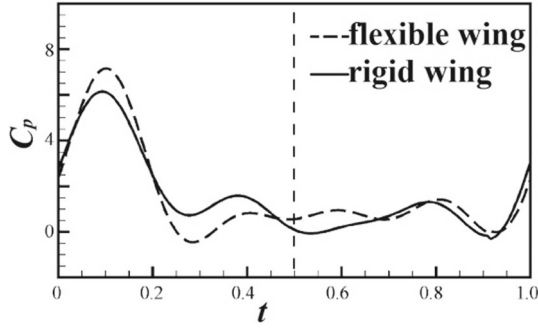


**Fig. 42** Predictions of the mechanical power production for both the flexible and rigid wings [72]

quantitative analysis as given in Fig. 41 clearly shows that production of both the vertical force and thrust by the flexible wing is higher than those by the rigid wing.

In addition, Xu et al. [72] calculated power output requirement for both flexible and rigid wings and their results are plotted in Fig. 42. Even though higher power output is required for the flexible wing at several instants in time during one cycle, the values of output power averaged over the entire stroke cycle are quite close for the flexible and rigid wings. This result indicates that as a consequence of long-term evolution, the flexible wing does indeed have better energy efficiency than the rigid wing.

#### 4.3 Influence of shape of wing model

A smooth airfoil, an ellipse or a flat plate has been widely adopted in previous studies as the simplified shape of dragonfly wing profile. However, like other insects, dragonfly wings also exhibit a complex 3D corrugated wing structure that is shown in Fig. 37. Vargas et al. [75] numerically studied the effect of the dragonfly's corrugated wing structure on its aerodynamic characteristics in gliding dragonfly flight. In their simulations, three different wing modes which are given in Fig. 43 have been used.

Figure 44 shows the time-averaged streamlines generated by the pleated airfoil (Fig. 43a) at  $R_e = 10,000$ . It can be seen that a separation bubble is formed inside each of the air gaps between pleat ends and trays. Inside the air gap, there are a point of separation at just the downstream side of the pleat tip and a point of flow reattachment at the upstream side of the successive pleat tip, so that several small regions of recirculating flow are formed along the surface of the pleated airfoil (see Fig. 44). Vardas et al. further compared the flow

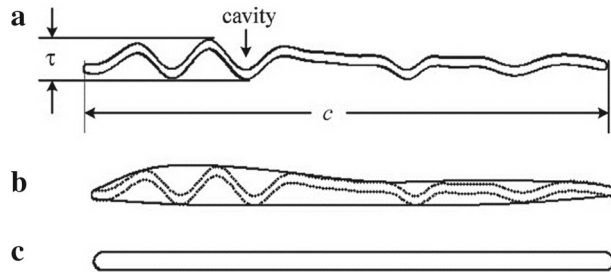


**Fig. 43** The shapes of wing model studied by Vargas et al. [75]: **a** corrugated airfoil representing a cross section of the forewing of a dragonfly (*Aeshna cyanea*) with  $\tau/c = 7.531\%$ ; **b** profile of an airfoil formed by the pleated airfoil whose local extrema are connected and  $\tau/c = 7.531\%$ ; **c** flat plate with  $\tau/c = 3.342\%$

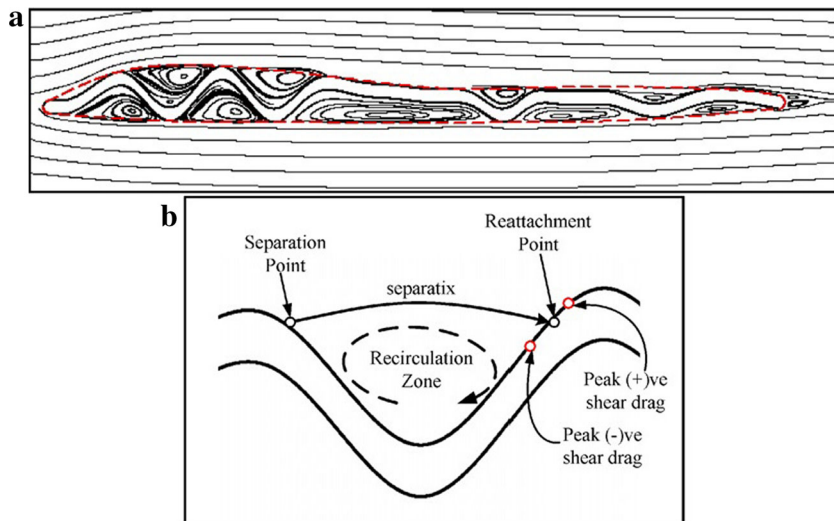


**Fig. 44** **a** The computed flow pattern around the corrugated airfoil and **b** the vortex trapped inside the air gap between adjacent pleat structures of the dragonfly wing [75]

fields generated by the profiles of the cross sections (a), (b) and (c) that was proposed in Figure 43. Based on the comparison results gained in Fig. 45, they found that the air flow pattern around the wing at different Reynolds number is similar for all three different dragonfly wing sections.

Nevertheless, detailed quantitative analysis of the forces on the wings in Fig. 46 shows the expected differences in the values of lift and drag coefficient between the three different wing shapes. For all three wing shapes, the drag force coefficient is monotonically decreased with increasing Reynolds number. Except for the flat plate whose lift coefficient has an apparent peak, the lift curve for the pleated airfoil and profiled airfoil, however, behaves in a similar manner and the lift coefficient increases with an increase in Reynolds number. It thus seems feasible, in principle, to use the simplified model instead of the natural structure of a dragonfly wing to study the aerodynamics of the wing, as the simplified model can give a clear physical picture and also make the theoretical analysis as well as the experimental performance more convenient. However, if the accurate quantitative analysis is required, the correction should be applied to the data obtained by the use of the simplified wing model in order to include the effect of the wing corrugation on its aerodynamic performance.

#### 4.4 Influence of aerodynamic models of flapping wing motions

As mentioned earlier, two-dimensional (2D) wing models are being widely used by investigators to study the aerodynamic behavior of flapping wings. However, the 2D model is not accurate enough for predictions of aerodynamic forces on flapping wings. Although a 2D model is sufficient to capture characteristics of flapping wing kinematics during downstroke, the wing's angle of attack during the upstroke is usually not able to be precisely determined by using a 2D model. In addition, three-dimensional wing characteristics of the dragonfly

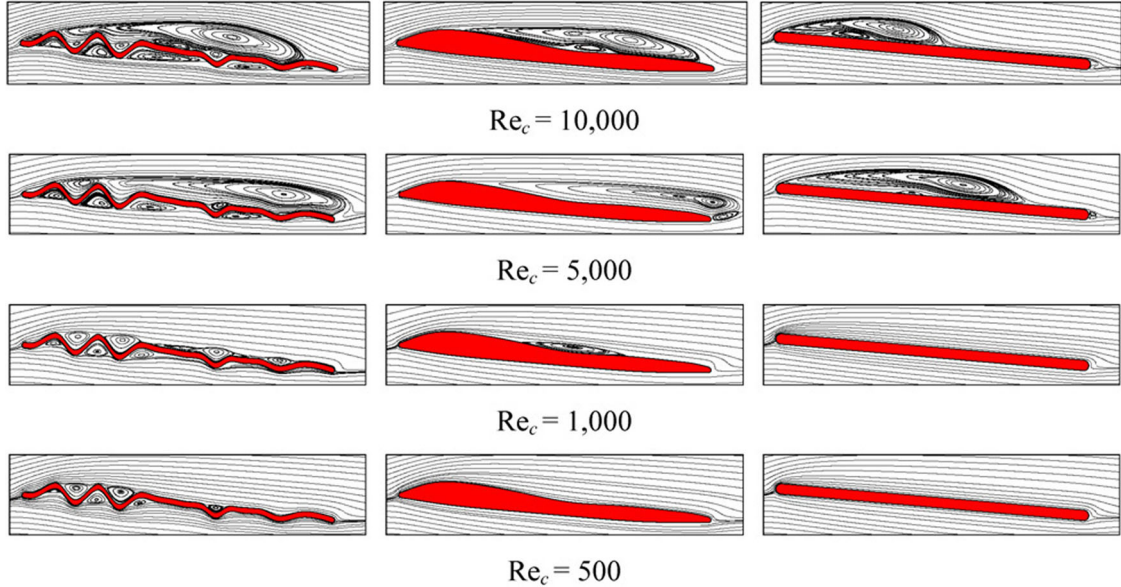


**Fig. 45** Flow patterns, respectively, generated by three different dragonfly wing sections at different Reynolds number [75]

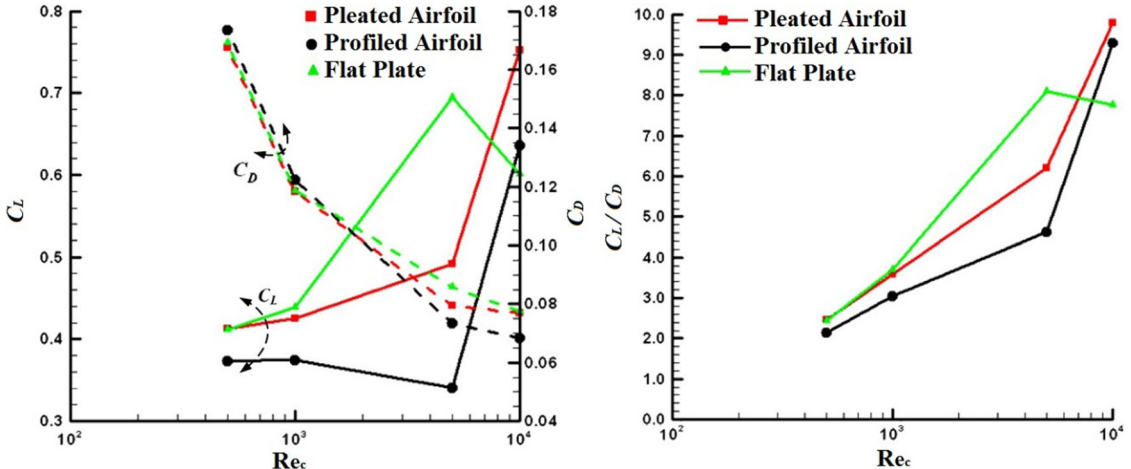


**Fig. 46** The variation of lift coefficient ( $C_L$ , the solid line), drag coefficient ( $C_D$ , the dash line) and lift-to-drag ( $C_L/C_D$ ) with Reynolds number for the three wing shapes [75]

might yield profound three-dimensional effects in the unsteady flows produced by the dragonfly. When the spacing between fore- and hindwings increases along the span of the wing, the interactions between the wings become weakened. Conversely, 2D tandem wings might aggravate this effect of wing–wing interactions in dragonfly flight and cause the numerical results to be less accurate.

A few models have been proposed to describe the motion of a three-dimensional rigid wing in flapping and pitch motion. Except for the model which has been used in forward flight studies and introduced in Sect. 3.4, another common model that has been applied has the following forms [41]:

$$\varphi = 0.5\Phi \left[ 1 - \cos \left( \frac{2\pi t}{T} + \psi \right) \right] \quad (18)$$

$$\rho(t) = \begin{cases} \rho_M \sin(\pi t / \Delta T_r), & 0 \leq t \leq 0.2T \\ \rho_M, & 0.2T \leq t \leq 0.3T \\ \rho_M \cos[\pi(t - 0.3T) / \Delta T_r], & 0.3T \leq t \leq 0.7T \\ -\rho_M, & 0.7T \leq t \leq 0.8T \\ -\rho_M \cos[\pi(t - 0.8T) / \Delta T_r], & 0.8T \leq t \leq T \end{cases} \quad (19)$$

Equation (18) is the kinematic function of translation including the azimuthal rotation of the wing about the translational axis and the plane on which the model wing translates.  $\psi$  is the phase difference between the flapping motions of the fore- and hindwings at the initial time point.  $\psi$  can be different for different flight modes of a dragonfly, for example,  $\psi = 0$  for forewing and  $\psi = \pi$  for hindwing during hovering flight. Equation (19) is the kinematic function of rotation, in which  $\rho_M$  is the maximal rotational angle and  $T$  is the time to perform one complete stroke cycle.

These models have been proposed based principally on experimental observations. So far there are not enough data to suggest which model may have broader applicability or provide more precise predictions.

## 5 Discussions and conclusions

Based on a review of the existing literature, this paper attempts to summarize and review the recent research and developments in the study of dragonfly flight dynamics. Among the issues considered, special attention is given to the aerodynamic explanation for some of the phenomena of the flapping flight of the dragonfly.

Recent research findings show that acceleration flight, low-speed forwarding flapping flight or hovering flight depends on vortex dominated unsteady aerodynamics, by which the high vertical forces on the dragonfly's wings required to generate these maneuvers can be produced. With the increase of the speed of forward flight, the leading-edge vortex formed on the wings progressively evolves into a thin separation layer which is pressed closely to the surface of the wing. In this way, higher values of thrust and vertical force can be yielded to meet the need of flight stability at high forward speed. During flight, it is found that there are two peak values of the total vertical force over one complete flapping cycle and these two peaks are generated during the downstroke movement of fore- and hindwings, respectively. Moreover, the time interval between peaks changes with varying phase difference between the cycles of the fore- and hindwings. When there is a phase difference of  $0^\circ$  (both wings flapping together), the two peaks have merged into a single peak whose value is comparatively much higher, and in this case, the dragonfly is accelerating itself in one direction. For both the forewing and hindwing, the rotational motion of the upstrokwing might cause other small peaks of the vertical force coefficient in addition to the one strong peak occurred during the downstroke phase. Through analysis of the power consumed by a flying dragonfly, it is interesting to note that the dragonfly may also be able to use the rotational motion of its wings to harness the energy from the moving air for the purpose of energy saving.

In a tandem wing configuration, active manipulation of the phase difference between the fore- and hindwings is one of the most apparent methods of flight control. A  $180^\circ$  phase difference which is accepted by researchers as the most typical value is usually used for the study of the hovering flight of the dragonfly. However, some researchers found that a  $90^\circ$  phase difference is also used by the dragonfly for hovering. As changes in the phase angle between the flapping motions of the fore- and hindwings have a relatively small effect on the flow phenomena around the wing of a hovering dragonfly, the phase difference ranging from about  $55^\circ$  to almost  $180^\circ$  all has been found in some studies on aerodynamic mechanism of hovering flight of dragonfly. Furthermore, apart from a  $90^\circ$  phase difference, a  $180^\circ$  phase difference is also used for straight forward flight. Researchers can merely confirm that the phase difference selected in their studies is appropriate for the flight mode of the dragonfly being studied. However, it is still not certain whether the relative position between the wings remains unchanged for a dragonfly flying a specific maneuver.

Earlier studies were often conducted on tethered dragonflies because of the limitations of computational and experimental methods in earlier phases. Therefore, even though the spatial position of the tested dragonfly seems not changed, this is not a hovering dragonfly under natural conditions and in fact is a dragonfly in escape mode. This behavior difference should be kept in mind when comparing the results of the early studies with those of recent research.

There are approximately 3600 known species of dragonfly in the world which display an uneven global distribution. So far, only a few species have been studied. However, different species result in differences in wing-aspect ratio and wing shape. Consequently, the phase relationship of their wing movement also varies. It might be interesting to identify the differences in aerodynamic performance resulting from subtle structural differences, which are certainly conducive to the development of biomimetic micro-air vehicles built based on flapping wing aerodynamics.

Some researchers have noticed the flight characteristics difference caused by the use of different wing shapes in the simulation of hovering flight of the dragonfly. However, it is necessary to provide comprehensive studies to identify the influence of the wing shape on the simulation results in other flight modes of a dragonfly. In addition, it has been proposed by some that the wing corrugation varies at different positions along the span

of a wing of a dragonfly, and this mode has been shown to have results which closely match actual wings' behavior. However, the aerodynamic properties of different corrugation patterns should be studied further.

It is no doubt that an exploration of the dragonfly flight mechanism will serve as a guide to further development of microair vehicles. However, there are essential differences between the real dragonfly and man-made micro-air vehicles, including wing material, composition and function of insect flight muscle and mechanical transmission system. The key kinematic parameters such as the maximum flapping frequency, the maximum allowable wing speed and the maximum allowable weight should be considerably different for them. Therefore, a better understanding and characterization of real dragonfly flight can only provide a valuable reference for researchers, but should not have a decisive effect upon the further development of MAVs, due to the difference between biological tissues and man-made materials. The flapping wing motions of MAVs could be optimized based on the flight patterns of flying dragonflies. Hence, interdisciplinary collaboration of engineering and the life sciences becomes critically important to bring our own creations closer to the perfection of nature.

With the rapid development of computer hardware, CFD modeling is certain to become a more important tool to understand the fluid dynamic phenomena underlying the flapping wings of a dragonfly. Although 2D CFD models were used originally, 3D models are better suited to represent the flow field generated by a flapping wing which is highly three dimensional and time varying. However, high-resolution simulations require enormous computational resources. Although a great deal of computation time and expense could be saved by the continued advancement of computer technologies, development of the appropriate numerical modeling approach and grid generation methods is especially important as well in precisely capturing flying activity. In order to validate the numerical results, experimental observations and measurement will continue to play an essential role in further understanding of the dragonfly aerodynamics. It is of interest to extend the observations made by previous studies by performing a more precise measurement of the flowfield in order to gain more spatial and temporal information on the aerodynamic properties and flow structures of flow field between two wings in tandem arrangement.

**Acknowledgements** This work was supported by National Natural Science Foundation of China Grant (Nos. 50836006, 11202123 and 51376096).

## References

- Ellington, C.P.: The novel aerodynamics of insect flight: applications to micro-air vehicles. *J. Exp. Biol.* **202**, 3439–3448 (1999)
- Obata, A., Shinohara, S., Akimoto, K., Suzuki, K., Seki, M.: Aerodynamic bio-mimetics of gliding dragonflies for ultra-light flying robot. *Robotics* **3**, 163–180 (2014)
- Couceiro, M.S., Fonseca Ferreira, N.M., Tenreiro Machado, J.A.: Analysis and control of a dragonfly-inspired robot. In: International Symposium on Computational Intelligence for Engineering Systems, Porto, pp. 18–19 (2009)
- Couceiro, M.S., Fonseca Ferreira, N.M., Tenreiro Machado, J.A.: Hybrid adaptive control of a dragonfly model. *Commun. Nonlinear Sci. Numer. Simul.* **17**, 893–903 (2012)
- Hu, Z., Deng, X.Y.: A flight strategy for intelligent aerial vehicles learned from dragonfly. In: Lam, T.M. (ed.) *Aerial Vehicles*, pp. 189–202. InTech, Rijeka (2009)
- Gaisser, N., Mugrauer, R., Mugrauer, G., Jebens, A., Jebens, K., Knubben, E.M.: Inventing a micro aerial vehicle inspired by the mechanics of dragonfly flight. In: Natraj, A., Cameron, S., Melhuish, C., Witkowski, M. (eds.) *Towards Autonomous Robotic Systems*, pp. 90–100. Springer, Berlin (2014)
- Azuma, A., Azuma, S., Watanabe, I., Furuta, T.: Flight mechanics of a dragonfly. *J. Exp. Biol.* **116**, 79–107 (1985)
- Azuma, A., Watanabe, T.: Flight performance of a dragonfly. *J. Exp. Biol.* **137**, 221–252 (1988)
- May, M.L.: Dragonfly flight: power requirement at high speed and acceleration. *J. Exp. Biol.* **158**, 325–342 (1991)
- Wakeling, J.M., Ellington, C.P.: Dragonfly flight. I. Gliding flight and steady-state aerodynamic forces. *J. Exp. Biol.* **200**, 543–556 (1997)
- Wakeling, J.M., Ellington, C.P.: Dragonfly flight. II. Velocities, accelerations and kinematics of flapping flight. *J. Exp. Biol.* **200**, 557–582 (1997)
- Wakeling, J.M., Ellington, C.P.: Dragonfly flight. III. Lift and power requirements. *J. Exp. Biol.* **200**, 583–600 (1997)
- Alexander, D.E.: Wind tunnel studies of turns by flying dragonflies. *J. Exp. Biol.* **122**, 81–98 (1986)
- Alexander, D.E.: Unusual phase relationships between the forewings and hindwings in flying dragonflies. *J. Exp. Biol.* **109**, 379–383 (1984)
- Alexander, D.E.: Studies on flight control and aerodynamics in dragonflies. 1982, PhD Dissertation, Duke University
- Freymuth, P.: Thrust generation by an airfoil in hover modes. *Exp. Fluids* **9**, 17–24 (1990)
- Chadwick, L.E.: The wing motion of the dragonfly. *Bull. Brooklyn Ent. So.* **35**, 109–112 (1940)
- Neville, A.C.: Aspects of flight mechanics in anisopterous dragonflies. *J. Exp. Biol.* **37**, 631–656 (1960)
- Newman, B.G., Savage, S.B., Schouella, D.: Model tests on a wing section of an *Aeschna* dragonfly. In: Pendley, T.J. (ed.) *Scale Effects in Animal Locomotion*, pp. 445–477. Academic Press, New York (1977)

20. Norberg, R.A.: Hovering flight of the dragonfly *Aeschna juncea* L., kinematics and aerodynamics. In: Wu, Y.T., Brokaw, C.J., Brennen, C. (eds.) *Swimming and Flying in Nature*, vol. 2, pp. 763–781. Plenum Press, New York (1975)
21. Russell, D.B.: Numerical and experimental investigations into the aerodynamics of dragonfly flight. Cornell University, New York Thesis (Ph.D.), (August, 2004)
22. Wang, Z.J., Russell, D.B.: Effect of forewing and hindwing interactions on aerodynamic forces and power in hovering dragonfly flight. *Theoret. Appl. Mech.* **148***101*, 1–4 (2007)
23. Thomas, A.L., Taylor, G.K., Srygley, R.B., Nudds, R.L., Bomphrey, R.J.: Dragonfly flight: free-flight and tethered flow visualizations reveal a diverse array of unsteady lift-generating mechanisms, controlled primarily via angle of attack. *J. Exp. Biol.* **207**, 4299–4323 (2004)
24. Wang, Z.J.: Vortex shedding and frequency selection in flapping flight. *J. Fluid Mech.* **410**, 323–341 (2000)
25. Wang, Z.J.: Two dimensional mechanism for insect hovering. *Phys. Rev. Lett.* **85**, 2035–2038 (2000)
26. Wang, Z.J., Birch, J.M., Dickinson, M.H.: Unsteady forces and flows in low Reynolds number hovering flight: two dimensional computations vs robotic wing experiments. *J. Exp. Biol.* **207**, 449–460 (2004)
27. Wu, J.H., Sun, M.: Unsteady aerodynamic forces of a flapping wing. *J. Exp. Biol.* **207**, 1137–1150 (2004)
28. Sun, M., Hamdani, H.: A study on the mechanism of high-lift generation by an airfoil in unsteady motion at low Reynolds number. *Acta Mech. Sin.* **17**, 97–114 (2001)
29. Mou, X.L., Sun, M.: Effects of wing planform on aerodynamic force production of stroking model insect wing. *J. Beijing Univ. Aeronaut. Astronaut.* **37**, 1359–1364 (2011)
30. Lan, S., Sun, M.: Aerodynamic properties of a wing performing unsteady rotational motion at low Reynolds number. *Acta Mech.* **149**, 145–147 (2001)
31. Lan, S., Sun, M.: Aerodynamic force and flow structures of two airfoils in flapping motions. *Acta Mech. Sin.* **17**, 310–331 (2001)
32. Lehmann, F.O.: Wing–wake interaction reduces power consumption in insect tandem wings. *Exp. Fluids* **46**, 765–775 (2009)
33. Gustafson, K., Leben, R.: Computation of dragonfly aerodynamics. *Comput. Phys. Commun.* **65**, 121–132 (1991)
34. Resh, V.H., Cardé, R.T.: *Encyclopedia of Insects*. Academic Press, San Diego (2009)
35. Berman, G., Wang, Z.J.: Energy-minimizing kinematics in hovering insect flight. *J. Fluid Mech.* **582**, 153–168 (2007)
36. Lu, Y., Shen, G.X., Lai, G.J.: Dual leading-edge vortices on flapping wings. *J. Exp. Biol.* **209**, 5005–5016 (2006)
37. Premachandran, S., Giacobello, M.: The effect of wing corrugations on the aerodynamic performance of low-Reynolds number flapping flight. In: 17<sup>th</sup> Australasian Fluid Mechanics Conference. Auckland, New Zealand. 5–9 December, 2010
38. Sudhakar, Y., Vengadesan, S.: Flight force production by flapping insect wings in inclined stroke plane kinematics. *Comput. Fluids* **39**, 683–695 (2010)
39. Wang, Z.J.: Dissecting insect flight. *Ann. Rev. Fluid Mech.* **37**, 183–210 (2005)
40. Wang, H., Zeng, L.J., Liu, H., Yin, C.Y.: Measuring wing kinematics, flight trajectory and body attitude during forward flight and turning maneuvers in dragonflies. *J. Exp. Biol.* **206**, 745–757 (2003)
41. Lai, G.J., Shen, G.X.: Experimental investigation on the wing–wake interaction at the mid stroke in hovering flight of dragonfly. *Sci. China Phys. Mech. Astron.* **55**, 2167–2178 (2012)
42. Wang, J.K., Sun, M.: A computational study of the aerodynamics and forewing–hindwing interaction of a model dragonfly in forward flight. *J. Exp. Biol.* **208**, 3785–3804 (2005)
43. Sane, S.P.: The aerodynamics of insect flight. *J. Exp. Biol.* **206**, 4191–4208 (2003)
44. Shyy, W., Trizila, P., Kang, C., Aono, H.: Can tip vortices enhance lift of a flapping wing? *Aerosp. Lett.* **47**, 289–293 (2009)
45. Hefler, C., Qiu, H., Shyy, W.: The interaction of wings in different flight modes of a dragonfly. 17<sup>th</sup> International Symposium on Application of Laser Techniques to Fluid Mechanics. Lisbon, Portugal (07–10 July, 2014)
46. Alexander, D.E.: Unusual phase relationships between the forewings and hindwings in flying dragonflies. *J. Exp. Biol.* **109**, 379–383 (1984)
47. Newman, B.G., Savage, S.B., Schouella, D.: Model test on a wing section of an *Aeschna* dragonfly. In: Pedley, T.J. (ed.) *Scale Effects in Animal Locomotion*, pp. 445–477. Academic Press, London (1977)
48. Biewener, A.B.: *Animal Locomotion*. Oxford University Press, Oxford (2003)
49. Hankin, E.H.: The soaring flight of dragonflies. *Proc. Camb. Philos. Soc.* **20**, 460–465 (1921)
50. Polcyn, D.M.: The thermal biology of desert dragonflies. University of California, USA. Thesis (Ph.D.) (1988)
51. Corbet, P.S.: *A Biology of Dragonflies*. Classey, Farringdon (1983)
52. May, M.L.: Dependence of flight behavior and heat production on air temperature in the green darner dragonfly, *Anax junius* (Odonata: Aeshnidae). *J. Exp. Biol.* **198**, 2385–2392 (1995)
53. Zhang, J., Lu, X.Y.: Aerodynamic performance due to forewing and hindwing interaction in gliding dragonfly flight. *Phys. Rev. E* **80**, 017302 (2009)
54. Xiao, T.H.: A numerical method for unsteady low Reynolds number flows and application to Micro Air Vehicles. Nanjing University of Aeronautics and Astronautics, China, Thesis (Ph.D.) (April, 2009) (in Chinese)
55. Xiao, T.H., Ang, H.S.: Numerical study of unusual phase relationships and aerodynamic interaction between forewing and hindwing of dragonfly model. *Acta Aeronaut. ET Astronaut. Sin.* **30**, 1165–1175 (2009). (in Chinese)
56. Maybury, W.J., Lehmann, F.O.: The fluid dynamics of flight control by kinematic phase lag variation between two robotic insect wings. *J. Exp. Biol.* **207**, 4707–4726 (2004)
57. DiLeo, C., Deng, X.Y.: Design and experiments of a dragonfly-inspired robot. *Adv. Robot.* **23**, 1003–1021 (2009)
58. Guo, T.: Design and prototype of a hovering ornithopter based on dragonfly flight. Massachusetts Institute of Technology, USA. Bachelor's Thesis. (June, 2007)
59. Hu, Z., Deng, X.Y.: Aerodynamic effect of forewing–hindwing interactions in hovering and forward flight of dragonfly. In: Proceeding of the Annual Meeting of the Society for Integrative and Comparative Biology (SICB'09), Boston, USA (January, 2009)
60. Naidu, V., Young, J., Lai, J.C.S.: Effect of wing flexibility on dragonfly hover flight. In: 19th Australasian Fluid Mechanics Conference, Melbourne, Australia (December, 2014)

61. Hu, Z., McCauley, R., Schaeffer, S., Deng, X.: Aerodynamics of dragonfly flight and robotic design. In: Proceedings of the 2009 IEEE International Conference on Robotics and Automation, Kobe, Japan (May, 2009)
62. Ellington, C.P., Vandenberg, C., Willmott, A.P., Thomas, A.L.R.: Leading-edge vortices in insect flight. *Nature* **384**, 626–630 (1996)
63. Xie, C.M., Huang, W.X.: Vortex interactions between forewing and hindwing of dragonfly in hovering flight. *Theoret. Appl. Mech. Lett.* **5**, 24–29 (2015)
64. Hu, Z., Deng, X.Y.: Aerodynamic interaction between forewing and hindwing of a hovering dragonfly. *Acta Mech. Sin.* **30**, 787–799 (2014)
65. Sun, M., Lan, S.L.: A computational study of the aerodynamic forces and power requirements of dragonfly *Aeschna juncea* hovering. *J. Exp. Biol.* **207**, 1887–1901 (2004)
66. Sun, M., Tang, J.: Lift and power requirements of hovering flight in *Drosophila virilis*. *J. Exp. Biol.* **205**, 2413–2427 (2002)
67. Dokkum, P.V.: Dragonflies: Magnificent Creatures of Water, Air and Land. Yale University Press, New Haven (2015)
68. Berger, C.: Dragonflies. Stackpole Books, Mechanicsburg (2004)
69. Xu, J.L., Zhao, C.X., Zhang, Y.L., Zhang, Y.: Effect of flapping trajectories on the dragonfly aerodynamics. *Chin. Sci. Bull.* **51**, 777–784 (2006)
70. Jongerius, S.R., Lentink, D.: Structural analysis of a dragonfly wing. *Exp. Mech.* **50**, 1323–1334 (2010)
71. Chen, Y.H., Skote, M., Zhao, Y., Huang, W.M.: Stiffness evaluation of the leading edge of the dragonfly wing via laser vibrometer. *Mater. Lett.* **97**, 166–168 (2013)
72. Xu, M., Yu, Y.L., Bao, L.: Theoretical modeling study on the aerodynamic effects of dragonfly flexible wing in forward flapping flight. *J. Grad. Sch. Chin. Acad. Sci.* **23**, 729–735 (2006). (in Chinese)
73. Meng, L.B., Ang, H.S., Xiao, T.H.: Analysis of aerodynamic characteristics of flexible wing of dragonfly based on CFD/CSD method. *J. Aerosp. Power* **29**, 2063–2069 (2014). (in Chinese)
74. Nakata, T., Liu, H.: Aerodynamic performance of a hovering hawkmoth with flexible wings: a computational approach. *Proce. R. Soc. B* **279**, 722–731 (2011)
75. Vargas, A., Mittal, R., Dong, H.B.: A computational study of the aerodynamic performance of a dragonfly wing section in gliding flight. *Bioinspir. Biomim.* **3**, 026004 (2008)